Pharmacological Research 183 (2022) 106362

Contents lists available at ScienceDirect

Pharmacological Research

journal homepage: www.elsevier.com/locate/yphrs

Review

Janus kinase (JAK) inhibitors in the treatment of neoplastic and inflammatory disorders

Robert Roskoski Jr. *

Blue Ridge Institute for Medical Research, 3754 Brevard Road, Suite 106, Box 19, Horse Shoe, NC 28742, United States

ARTICLE INFO

Keywords:
Atopic dermatitis
Leukemia
Myelofibrosis
Polycythemia vera
Rheumatoid arthritis
STAT

Chemical compounds studied in this article:
Abrocitinib (PubChem CID: 78323835)
Baricitinib (PubChem CID: 44205240)
Belumosudil (PubChem CID: 11950170)
Fedratinib (PubChem CID: 16722836)
Fostamatinib (PubChem CID: 11671467)
Nintedanib (PubChem CID: 135423438)
Pacritinib (PubChem CID: 46216796)
Ruxolitinib (PubChem CID: 25126798)
Tofacitinib (PubChem CID: 9926791)
Upadacitinib (PubChem CID: 58557659)

ABSTRACT

The Janus kinase (JAK) family of nonreceptor protein-tyrosine kinases consists of JAK1, JAK2, JAK3, and TYK2 (Tyrosine Kinase 2). Each of these proteins contains a JAK homology pseudokinase (JH2) domain that interacts with and regulates the activity of the adjacent protein kinase domain (JH1). The Janus kinase family is regulated by numerous cytokines including interferons, interleukins, and hormones such as erythropoietin and thrombopoietin. Ligand binding to cytokine receptors leads to the activation of associated Janus kinases, which then catalyze the phosphorylation of the receptors. The SH2 domain of signal transducers and activators of transcription (STAT) binds to the cytokine receptor phosphotyrosines thereby promoting STAT phosphorylation and activation by the Janus kinases. STAT dimers are then translocated into the nucleus where they participate in the regulation and expression of dozens of proteins. JAK1/3 signaling participates in the pathogenesis of inflammatory disorders while JAK1/2 signaling contributes to the development of myeloproliferative neoplasms as well as several malignancies including leukemias and lymphomas. An activating JAK2 V617F mutation occurs in 95% of people with polycythemia vera and about 50% of cases of myelofibrosis and essential thrombocythemia. Abrocitinib, ruxolitinib, and upadacitinib are JAK inhibitors that are FDA-approved for the treatment of atopic dermatitis. Baricitinib is used for the treatment of rheumatoid arthritis and covid 19. Tofacitinib and upadacitinib are JAK antagonists that are used for the treatment of rheumatoid arthritis and ulcerative colitis. Additionally, ruxolitinib is approved for the treatment of polycythemia vera while fedratinib, pacritinib, and ruxolitinib are approved for the treatment of myelofibrosis.

1. Introduction to JAK-STAT signaling

The Janus kinase (JAK) family of non-receptor protein-tyrosine kinases consists of four members: JAK1, JAK2, JAK3, and TYK2 (Tyrosine Kinase 2) [1]. These proteins consist of seven distinct JAK homology (JH1-JH7) domains. These enzymes possess an inactive pseudokinase domain (JH2) amino-terminal to an active carboxyterminal protein kinase domain (JH1). The pseudokinase domain negatively regulates the functional protein kinase domain. Janus is a two-faced Roman God (looking forwards and backwards) whose name was given to this enzyme family because of the presence of two protein kinase domains within a single polypeptide chain. JAK was whimsically conceived as Just Another Kinase [2]. JAK1, JAK2, and TYK2 are expressed in almost all types of cells (excluding mature erythrocytes) whereas JAK3 is confined to hematopoietic, myeloid, and lymphoid cells [3]. Mature blood cells, which have a limited life span, are continuously renewed in an elaborate multistep process. The Janus kinases play an essential role in hematopoiesis; consequently, Janus kinase dysregulation can produce a wide variety of hematological illnesses. These protein kinases also function in many other processes such as metabolism, post-natal growth, and satiety (leptin signaling).

Manning et al. identified 478 classical and 40 non-classical or atypical human protein kinase family genes (total 518) that correspond to nearly 2% of the human protein-encoding genome [4]. Based upon

Abbreviations: ALL, acute lymphocytic leukemia; AML, acute myelogenous leukemia; AS, activation segment; CS or C-spine, catalytic spine; CL, catalytic loop; EGFR, epidermal growth factor receptor; HΦ or Φ, hydrophobic; IFNλR, interferon lambda receptor; IL, interleukin; JAK1/2/3, Janus kinases 1/2/3; JH, JAK homology; MW, molecular weight; PDGFR, platelet-derived growth factor receptor; PKA, protein kinase A; ΨK, pseudokinase; RA, rheumatoid arthritis; Ro5, Lipinski rule of 5; RS or R-spine, regulatory spine; Sh1, shell residue 1; STAT, signal transducer and activator of transcription; TNF, tumor necrosis factor; VEGFR, vascular endothelial growth factor receptor.

* Corresponding author.
E-mail address: rrj@brimr.org.

https://doi.org/10.1016/j.phrs.2022.106362
Received 20 July 2022; Accepted 20 July 2022
Available online 22 July 2022

the nature of the substrate –OH moiety, these catalysts are classified as protein-tyrosine kinases (90 members), tyrosine-kinase like enzymes (43), and protein-serine/threonine kinases (385). A small cadre of enzymes such as MEK1 and MEK2, which catalyze the phosphorylation of both tyrosine and then threonine residues of target proteins, are classified as dual specificity kinases. Of the 90 protein-tyrosine kinases, 58 are transmembrane receptor proteins and 32 are cytosolic non-receptor proteins, including the four members of the Janus kinase family. This enzyme family catalyzes the following reaction:

$$MgATP^{1-} + \text{protein-tyrosine–O:H} \rightarrow \text{protein-tyrosine–O:}PO_3^{2-} + MgADP + H^+$$

Note that it is the phosphoryl group (PO_3^{2-}) and not the phosphate (OPO_3^{2-}) that is transferred from ATP to a tyrosine residue within the protein substrate. Divalent cations such as Mg^{2+} or Mn^{2+} are required for the reaction for almost all protein kinases; however, Mg^{2+} is the physiological ion owing to its significantly greater intracellular content.

The JAK-STAT (signal transducer and activator of transcription) pathway conveys extracellular signals from a variety of cytokines, chemokines, growth factors, and hormones to the nucleus and is responsible for the expression of hundreds of protein-encoding genes [5]. Each of the Janus kinases binds to the intracellular juxtamembrane region of specific cytokine receptors. The genes specifying selected high-affinity cytokine receptor homo- or hetero-dimers are listed in Table 1. The cytokine receptors – which lack catalytic activity – consist of an extracellular domain, a transmembrane segment, and an intracellular domain that binds to specific Janus kinases.

Numerous actions are required for the transformation of an extracellular signal into a transcriptional response. First, ligand binding generates conformational changes in the cytokine receptors that lead to protein-tyrosine kinase activation as a result of the phosphorylation of two tyrosine residues within the activation segment of the JH1 domains as catalyzed by a partner Janus kinase JH1 enzyme. This intermolecular reaction is called phosphorylation in *trans*. Following activation, the JH1 protein kinase domains mediate the phosphorylation of cytokine

Table 1
Cytokine and growth factor stimulation of JAK-STAT signaling[a].

Cytokine/ hormone[b]	Genes of human receptor subunits	Downstream JAK dimers	Downstream STATs	Selected functions
Type I, common γ-chain (gene *IL2RG*) cytokines				
IL-2	*IL2RA/B-IL2RG*	JAK1 +JAK3	STAT3/5	Regulates T cell, B cell, and NK cell activities
IL-4	*IL4RA-IL2RG*	JAK1 +JAK3	STAT6	Induces differentiation of helper T cells; anti-inflammatory action on T cells and monocytes
IL-7	*IL7RA-IL2RG*	JAK1 +JAK3	STAT3/5	T cell development and homeostasis
IL-9	*IL9R-IL2RG*	JAK1 +JAK3	STAT1/3/5	T cell growth and differentiation
IL-15	*IL15RA-IL2RG*	JAK1 +JAK3	STAT3/5	Promotes T cell activation and proliferation
IL-21	*IL21R-IL2RG*	JAK1 +JAK3	STAT1/3/5	Down regulates NK cell activation
Type I, common β-chain (gene *CSF2RB*) cytokines				
GM-CSF	*CSF2RA-CSF2RB*	JAK2 +JAK2	STAT3/5	Growth of macrophages and granulocytes; stimulation and differentiation of stem cells; used to reverse neutropenia after chemotherapy
IL-3	*IL3RA/B-CSF2RB*	JAK2 +JAK2	STAT3/5/6	Differentiation of stem cells; proliferation of all cells in the myeloid lineage
IL-5	*IL5R-CSF2RB*	JAK2 +JAK2	STAT3/5/6	Stimulates B cell growth and immunoglobulin secretion
Type I, gp130 (gene *IL6RB* = *IL6ST*) cytokines				
IL-6	*IL6RA/B-IL6RB*	JAK1 +JAK2, JAK1 +TYK2	STAT1/3	Prototypic pro-inflammatory cytokine increases acute-phase protein production
IL-11	*IL11RA-IL6RB*	JAK1 +JAK2, JAK1 +TYK2	STAT3	Induces megakaryocyte colony formation and maturation
IL-27	*IL27RA-IL6RB*	JAK1 +JAK2, JAK1 +TYK2	STAT1/2/3/4/5	Regulation of B and T cell activity
Type I, heterodimeric cytokines				
IL-12 (35kD/ 40kD)	*IL12RB1-IL12RB2*	JAK1 +TYK2	STAT4	Induces T_H1 T helper cell formation
IL-23	*IL23R-IL12RB1*	JAK1 +TYK2	STAT3/4	Pro-inflammatory cytokine
Type I, hormone-like cytokines				
Erythropoietin	*EPOR-EPOR*	JAK2 +JAK2	STAT5	Control of red blood cell production; used to treat anemia
Thrombopoietin	*TPOR-TPOR*	JAK2 +JAK2	STAT1/3/5	Differentiation of megakaryocytes and platelets
G-CSF	*CSF3R-CSF3R*	JAK2 +JAK2	STAT5	Production of stem cells and granulocytes; used to treat neutropenia
Growth hormone	*GHR-GHR*	JAK2 +JAK2	STAT3/5a	Regulates post-natal body growth
Leptin	*LEPR-LEPR*	JAK2 +JAK2	STAT3/5a	Coordination of energy metabolism; increases satiety
Type II, IFN family cytokines				
IFN-α/β	*IFNAR1-IFNAR2*	JAK1 +TYK2	STAT1/2/4	Promotes antiviral activity; stimulates T cell, macrophage, and NK cell activity; used to treat multiple sclerosis
IFN-γ	*IFNGR1-IFNGR2*	JAK1 +TYK2	STAT1	Regulates macrophage and NK cell activation; used to treat chronic granulomatous disease and osteopetrosis
IL-28	*IFNLR1-IL10RB*	JAK1 +TYK2	STAT1/2/3/4/5	Enhances immunity against infection
IL-29	*IFNLR1-IL10RB*	JAK1 +TYK2	STAT1/2/3/4/5	Enhances immunity against infection
Type II, IL-10 family cytokines				
IL-10	*IL10RA-IL10RB*	JAK1 +TYK2	STAT3	Anti-inflammatory actions
IL-19	*IL20RA-IL20RB*	JAK1 +JAK2, JAK1 +TYK2	STAT3	B-cell activation
IL-20	*IL20RA-IL20RB*	JAK1 +JAK2, JAK1 +TYK2	STAT3	Regulates differentiation and proliferation of keratinocytes during inflammation
IL-22	*IL22RA1-IL10RB*	JAK1 +JAK2, JAK1 +TYK2	STAT1/3/5	Targets non-hematopoietic cells such as hepatocytes, keratinocytes, lung, and intestinal epithelial cells
IL-24	*IL20RA-IL20RB*	JAK1 +JAK2, JAK1 +TYK2	STAT1/3	Targets skin, lung, and reproductive cells
IL-26	*IL10RB-IL20RA*	JAK1 +JAK2, JAK1 +TYK2	STAT1/3	Enhances IL-10 secretion from monocytes and IL-8 secretion from macrophages

[a] Adapted from Ref. [5,6].
[b] G-CSF, granulocyte colony stimulating factor; GM-CSF, granulocyte-macrophage colony stimulating factor.

receptor tyrosine residues that attracts the SH2 domain of STATs. The activated JH1 domain then mediates the phosphorylation of the STAT molecules themselves. Such phosphorylated STATS then form dimers that are translocated into the nucleus where they mediate the transcription of target genes. Alternatively, STATs may preexist as dimers and phosphorylation may result in a conformational change that produces activation [7]. Janus kinase activation by EGFR and PDGF is downstream from the activated receptor and may involve other protein kinases such as Src [5,8].

Humans possess seven STAT genes that are labeled *STAT1, STAT2, STAT3, STAT4, STAT5A, STAT5B,* and *STAT6*. Each STAT protein contains six domains (from the N- to C-terminus) including an amino-terminal domain, a coiled-coil segment, a DNA-binding component, a linker segment, an SH2 domain, and a transcriptional activation domain (TAD), which were first described for STAT1 (Fig. 1 A) [9]. The transcriptional activation domain contains a tyrosine residue (Y) that is a substrate for an upstream Janus kinase. Following their phosphorylation, STATs forms homo- or heterodimers that result from the binding of a phosphotyrosine (pY) to the partner's SH2 domain. The dimer moves into the nucleus where it binds to DNA target sequences alone or in combination with other transcription factors that may enhance or repress DNA transcription.

The STATs have specific roles in signaling. For example, STAT1 participates in interferon, IL-10 family, thrombopoietin, and interleukin-9 (IL-9) signaling while STAT2 is chiefly involved in interferon-α/β and IL-28/29 signaling (Table 1). STAT3 participates in the signaling pathways initiated by many of the Type I, II, and IL-10 families of cytokines. Moreover, STAT4 plays a role in signaling by the Type I heterodimeric cytokines (IL-12/23) and Type II interferon family cytokines (IFN-α/β, IL-28/29). STAT5A/B participate in the signaling pathways initiated by Type I cytokines with common γ-chain or common β-chain receptor subunits as well as the hormone-like cytokines. Furthermore, STAT6 participates in IL-3/5 signaling. The material given in Table 1 is a general overview and the precise pathway from the stimulatory ligand and receptor to a definite Janus kinase and a specialized STAT depends upon the cellular milieu and physiological context.

The activity of all protein kinases is stringently regulated because of their general importance in various signaling pathways [10]. Multiple phosphoprotein phosphatases including PTP1B (protein tyrosine phosphatase), SHP1/2 (Sh2-containing phosphatase), and TCPTP (T-cell protein tyrosine phosphatase) mediate the dephosphorylation and inactivation of Janus kinases [7]. CD45 is a receptor phosphoprotein phosphatase that mediates the dephosphorylation of the activation segment phosphotyrosines of all four Janus kinases [11]. The SOCS (suppressor of cytokine signaling) family of eight proteins also

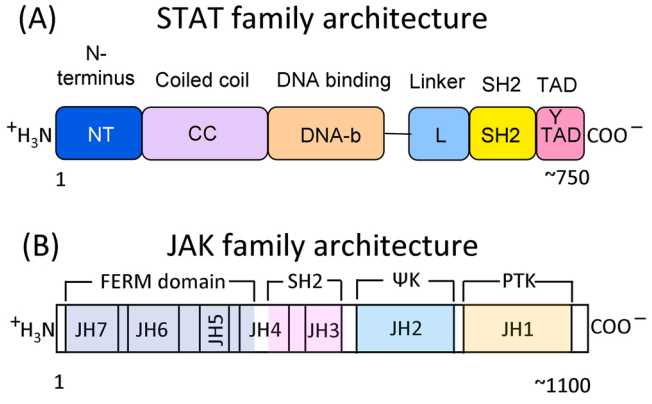

Fig. 1. (A) Overview of STAT architecture. TAD, transcriptional activation domain. (B) Overview of JAK-family architecture. ΨK, pseudokinase domain; PTK, protein-tyrosine kinase domain. The amino acid residue numbers are given at the base of the structures.

negatively regulates Janus kinase and cytokine signaling [5,7]. The SOCS proteins are ubiquitin ligases that mediate the proteasomal degradation of Janus kinase-associated cytokine receptors. Furthermore, SOCS1 and SOCS3 can bind to the protein-substrate binding grove within the kinase activation segment and sterically block the catalytic activity of JAK1/2 and TYK2, but not JAK3.

2. Janus kinase biochemistry

2.1. Janus kinase family architecture

The Janus kinases are large intracellular enzymes with about 1100 amino acid residues. They contain seven JAK homology modules listed as JH7-JH1 as we go from the amino-terminus to the carboxyterminus. These proteins are organized into four functional domains [12]. The amino-terminal JH7-JH6 module corresponds to a FERM domain (F for 4.1 protein, E for ezrin, R for radixin and M for moesin); this is a protein module consisting of ≈ 350 amino-acids and plays a role in targeting proteins to the plasma membrane. The JH5-JH3 module is an atypical SH2 domain that is unable to bind protein-tyrosine phosphate (it interacts with glutamate residues). The JH5-JH3 domain is followed by a JH2 pseudokinase domain and the carboxyterminal JH1 segment represents the functional protein-tyrosine kinase domain (Fig. 1B).

The Janus kinase JH2 and JH1 domains contain a small N-terminal lobe and large C-terminal lobe that contains several conserved α-helices and β-strands as first described by Knighton et al. for PKA in 1991 [13,14]. The N-terminal lobe is dominated by a twisted five-stranded antiparallel β-sheet (β1–β5) [15]. It also contains an important regulatory αC-helix (Fig. 2 A and D). The small lobe of the JAK2 JH1 domain contains a conserved glycine-rich (GEGHFG) ATP-phosphate-binding loop (GRL – sometimes called the P-loop), which occurs between the β1- and β2-strands. The signature sequence of this protein kinase loop is GxGxΦG, where x refers to any amino acid and Φ is a hydrophobic residue, usually phenylalanine or tyrosine. The β1- and β2-strands are located above the adenine base of ATP/ADP. The β3-strand generally contains an Ala-Xxx-Lys (AxK) sequence, the lysine of which (JAK2 K882) links the α- and β-phosphates of ATP/ADP to the αC-helix. A conserved glutamate residue is located near the center of the αC-helix (JAK2 E947) in protein kinases. The occurrence of a salt-bridge between the αC-glutamate and the β3-lysine is required for the formation of an active state, which corresponds to an "αC_{in}" conformation (Fig. 2 A). In contrast the K581 and E596 of the pseudokinase of the JAK2 JH2 domain fail to make contact, and this corresponds to an "αC_{out}" conformation (Fig. 2D). Moreover, the glycine-rich loop (GRL) in the JH2 domain consists of a shortened GRG sequence between the β1- and β2-strands. The αC_{in} conformation is necessary, but not sufficient, for the expression of full protein kinase activity.

The carboxyterminal lobe of the JAK protein kinase JH1 domains is mainly α-helical with six conserved segments (αD-αI), which occur in all protein kinases [15]. The large lobe also contains four short conserved β-strands (β6-β9). The primary structures of the β-strands are found between the αE- and αF-helices and include residues just before the catalytic loop (β6), after the catalytic loop and below the adenine ring of ATP (β7 and β8), and within the activation segment (β9). The activation segment of the JAK JH1 active state forms an open structure that allows protein binding (Fig. 2 A). In contrast, the activation segment of the dormant JH2 domain forms a closed, compact structure that sterically blocks protein binding (Fig. 2D).

In a comprehensive analysis, Hanks and Hunter identified 12 subdomains (I–VIa, VIb–XI) with signature sequences that constitute the regulatory and catalytic residues of protein kinases [16]. The following four amino acids, which are part of a K/E/D/D core, characterize the mechanistic properties of the JAK2 JH1 protein-tyrosine kinase domain. An invariant β3-strand lysine (K882, the K of K/E/D/D) forms a salt bridge with the αC-glutamate (E898, the E of K/E/D/D) and also the α- and β-phosphate groups of ATP/ADP (Fig. 2B). The catalytic loop

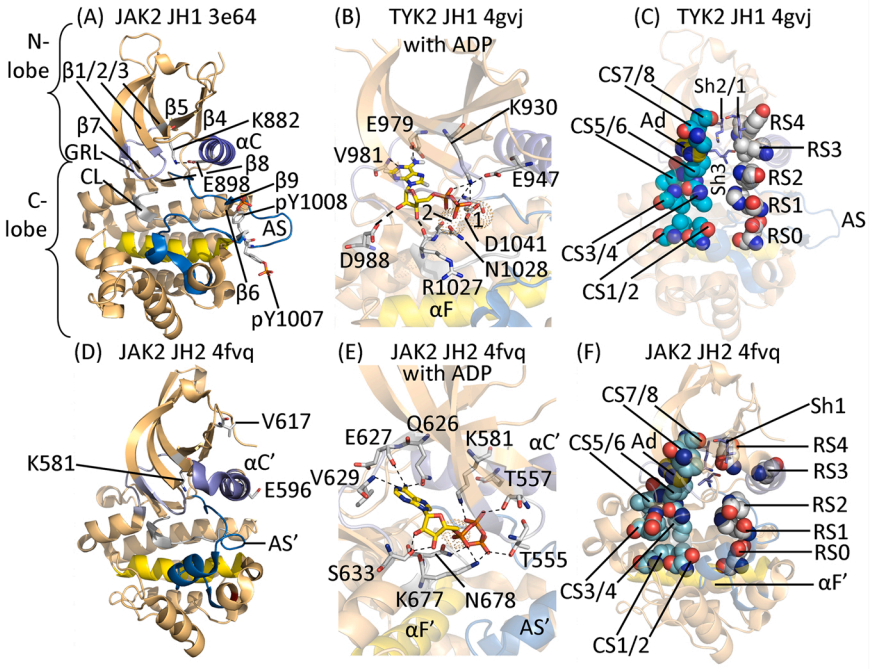

Fig. 2. (A) The active JAK2 JH1 protein-tyrosine kinase domain. (B) ADP bound to the active TYK2 JH1 domain. (C) Spine and shell residues of the active TYK2 JH1 domain. (D) The inactive JAK2 JH2 ΨK domain. (E) ADP bound to the inactive JAK2 JH2 domain. (F) Spine and shell residues of the inactive JAK2 JH2 domain. Ad, adenine; AS, activation segment, CL, catalytic loop; GRL, glycine-rich loop. Dashes designate polar bonds. The four-letter PDB ID is provided with each depiction. Figs. 2, 3, 4B, and 7 were prepared using the PyMOL Molecular Graphics System Version 1.5.0.4 Schrödinger, LLC.

surrounding the actual site of phosphoryl transfer consists of HRDLAARN in JAK1, JAK3 and TYK2; the sequence HRDLATRN occurs in JAK2. The JAK1 JH2 pseudokinase domain contains HGNVCTKN. The catalytic aspartate in JAK2 (D976), which is the first D of K/E/D/D, serves as a base that accepts a proton from the tyrosyl –OH moiety. This residue in the pseudokinase domains of the Janus kinases is an asparagine, which cannot accept a proton from the phenolic hydroxyl, thereby contributing to the catalytic dormancy of the pseudokinase domains. The AAR sequence in the catalytic loop is a receptor protein-tyrosine kinase signature and RAA is a non-receptor protein kinase signature; the existence of AAR in the JAK non-receptor protein kinases is thus anomalous.

The second aspartyl residue of the K/E/D/D signature of JAK2 (D994) is the first residue of the activation segment. The activation segment of almost all protein kinases including the Janus kinases begins with DFG (Asp-Phe-Gly) and ends with APE (Ala-Pro-Glu) or a related triad signature such as PPE. DFG-D1041 binds Mg^{2+}(1), which in turn interacts with the α- and β-phosphates of ATP/ADP. The HRDxxxxN (N1028) binds Mg^{2+}(2), which in turn interacts with the α- and γ-phosphates of ATP. In the active conformation, the DFG-D is directed inward toward the active site (DFG-D_{in}) where it can bind Mg^{2+}(1). In contrast, when the DFG-D is pointed outward, the resulting DFG-D_{out} structure is catalytically impaired owing to the blockade of ATP and protein substrate binding. The 6-amino portion of ATP generally forms a hydrogen bond with the C═O backbone residue of the first hinge residue (E979 of the JAK1 JH1 domain) that connects the N- and C-lobes of the protein kinase domain and the N1 nitrogen of the adenine moiety hydrogen bonds with the N–H group of the third hinge residue (V981) (Fig. 2B). As considered later, most steady-state ATP competitive small molecule Janus kinase inhibitors also make hydrogen bonds with the backbone residues of the connecting hinge. The end of the activation segment of the carboxyterminal lobe generally binds and positions the protein substrates.

The activation segment is an important mediator of protein-substrate binding and catalysis [17]. This segment in Janus kinases contains two phosphorylatable tyrosines (Fig. 2 A) [18]. The activation segment is located near the N-terminus of the αC-helix and the HRD signature of the catalytic loop. These components interact hydrophobically. As for most protein kinases [10], phosphorylation of residues within the activation segment shifts the equilibrium from an inactive JAK JH1 domain to an active one [19]. Several important human Janus kinase JH1 residues are listed in Table 2.

2.2. Hydrophobic spines in active JH1 and inactive JH2 domains

Kornev et al. analyzed the structures of functional and dormant conformations of 23 protein kinases and they discovered the role of essential residues by a local spatial pattern alignment algorithm [20,21]. Their analysis led to a classification of four hydrophobic residues that constitute a regulatory or R-spine and eight hydrophobic residues that make up a catalytic or C-spine. The adenine portion of ATP is one component of the catalytic spine. Each spine consists of amino acids that are found in both the small and large lobes. The regulatory spine contains a residue from the αC-helix and the activation segment, both of which are important in determining functional and inactive states. The R-spine participates in the placement of the protein substrate and the C-spine positions ATP to enable catalysis. The structure of the spines differs between the active JH1 and dormant JH2 domains. Moreover, the correct alignment of both the R-and C-spines is necessary for the assembly of an active protein kinase JH1 domain.

The protein kinase R-spine signature consists of the phenylalanine of the activation segment DFG, the histidine of the catalytic loop HRD, the amino acid four residues carboxyterminal to the conserved αC-glutamate of the αC-helix, and a residue at the N-terminus of the β4-strand. The backbone of the HRD-H is anchored to the very hydrophobic αF-helix by a hydrogen bond to a conserved aspartate side chain. Going from the αF-helix aspartate to the top residue of the spine within the β4-strand, Meharena et al. named the R-spine residues RS0, RS1, RS2, RS3, and RS4 (Fig. 2 C and 2 F) [17]. The R-spine of the functional JH1 protein kinase domain is nearly linear while that of the dormant JH2 pseudokinase domain is broken with RS3 displaced.

The protein kinase catalytic spine is made up of residues from both the amino-terminal and carboxyterminal lobes; the C-spine is completed by the adenine moiety of ATP (Fig. 2 C) [17,21]. The two small lobe residues of protein kinase domains that bind to the adenine base of ATP include a valine at the beginning of the β2-strand (CS7) and an alanine from the conserved AxK of the β3-strand (CS8). Additionally, a hydrophobic residue from the β7-strand (CS6) interacts with the adenine ring

Table 2
Important residues in human and selected mouse (m) JAK family members.

	JAK1	JAK2	JAK3	TYK2	mJAK1	Inferred function	Hanks no.
FERM domain	34–420	37–380	24–356	26–431	34–420	Interacts with receptor	–
SH2-like	439–544	410–482	375–475	450–529	439–542	Binds glutamate	–
ΨK	583–855	545–809	521–781	589–875	582–854	Regulation	–
PTK	875–1153	849–1124	822–1111	897–1176	874–1152	Catalysis	–
N-Lobe							
Glycine-rich loop: GxGxΦG	^{882}GEGHFG^{887}	^{856}GKGNFG^{861}	^{829}GKGNFG^{834}	^{904}GEGHFG^{909}	^{882}GEGHFG^{887}	Anchors ATP β-phosphate	I
β3-K (K of K/E/D/D)	K908	K882	K855	K930	K908	Forms ion pair with ATP α- and β-phosphates	II
αC-E (E of K/E/D/D)	E925	E898	E871	E947	E925	Forms ion pair with β3-K	III
Hinge residues	^{957}EFLPG^{961}	^{931}YKPYG^{936}	^{903}EYLPSG^{908}	^{979}EYVPLG^{984}	^{957}EFLPG^{961}	Connects N- and C-lobes	V
C-Lobe							
αE-AS loop and AS HΦ-interaction	Y999–A1027	Y972–V1000	C945–L973	Y1019–A1047	Y998–A1026	Stabilizes AS	VIb-VII
Catalytic loop HR*D* (first *D* of K/E/*D*/D)	D1003	D976	D949	D1023	D1003	Catalytic base (abstracts proton)	VIb
Catalytic loop Asn (N)	N1008	N981	N954	N1028	N1008	Chelates Mg^{2+}(2)	VIb
Activation segment	1021–1051	994–1024	967–997	1041–1071	1021–1051	Positions protein substrate	VII-VIII
AS *D*FG (second *D* of K/E/D/*D*)	D1021	D994	D967	D1041	D1021	Chelates Mg^{2+}(1)	VII
AS phosphorylation site	Y1034/Y1035	Y1007/Y1008	Y980/Y981	Y1054/Y1055	Y1034/Y1035	Stabilizes the AS after phosphorylation	VIII
APE, end of AS	1049–1051	1022–1024	995–997	1069–1071	1049–1051	Interacts with the αHI loop and stabilizes the AS	VIII
JH7	44–117	51–124	37–110	40–113	44–117	FERM domain	–
JH6	147–180	142–170	126–154	141–169	147–180	FERM domain	–
JH5	309–324	282–299	265–282	310–327	309–324	FERM domain	–
JH4	378–452	329–411	304–387	389–462	378–452	FERM + SH2 like	–
JH3	500–550	455–506	432–482	508–558	500–550	SH2 like	–
JH2	583–855	545–809	521–781	589–875	582–854	Pseudokinase	–
JH1	875–1153	849–1124	822–1111	897–1176	874–1152	Protein-tyrosine kinase	–
UniProt KB ID	P23458	O60674	P52333	P29597	P23458		

[a]AS, activation segment; Φ, hydrophobic residue.

system. This CS6 residue is flanked by two hydrophobic residues designated CS4 and CS5 that interact with the CS3 residue near the beginning of the αD-helix. Finally, the CS3 and CS4 residues interact hydrophobically with the CS1 and CS2 residues of the αF-helix to produce a completed C-spine [22]. Of significance, the hydrophobic αF-helix anchors both the R- and C-spines. Furthermore, the spines play an important role in positioning the protein kinase catalytic residues in their active and functional state. When comparing the locations of the spinal residues, the greatest divergence in the structures of the JH1 and JH2 domains involve RS3 and RS4 (Fig. 2 C and 2 F).

Based upon site-directed mutagenesis experiments, Meharena et al. identified three residues in murine PKA that stabilize the regulatory spine that they labeled Sh1, Sh2, and Sh3, where Sh refers to shell [17]. Sh2 is the gatekeeper residue. The term gatekeeper describes the role that this residue plays in restricting access to the back cleft. The back cleft is also called hydrophobic pocket II (HPII) or the back pocket. The residues that form the spines were identified by their locations in functional and dormant enzymes based upon their X-ray crystallographic three-dimensional structures [20,21]. This contrasts with the classification of the HRD, DFG, or APE amino acid signatures based upon their primary structures [16]. A summary of the spine and shell residues of the JAK JH1 and JH2 domains is given in Table 3. Therapeutic small molecule protein kinase inhibitors generally interact with residues that make up the C-spine and shell residues and sometimes those of the

Table 3
Spine and shell residues of selected murine (m) and human Janus kinase and pseudokinase (Ψ) domains.

	Symbol	KLIFS No.	mJAK1 Ψ	mJAK1	JAK1 Ψ	JAK1	JAK2 Ψ	JAK2	JAK3 Ψ	JAK3	TYK2 Ψ	TYK2
Regulatory spine												
β4-strand (N-lobe)	RS4	38	L652	Y939	L653	Y940	N612	Y913	L587	Y886	V673	Y962
C-helix (N-lobe)	RS3	28	M640	L928	M641	L929	M600	L902	L575	L875	L661	L951
Activation loop DFG-F (C-lobe)	RS2	82	P739	F1021	P740	F1022	P700	F995	P672	F968	P760	F1042
Catalytic loop HRD-H (C-lobe)	RS1	68	H711	H1000	H712	H1001	H671	H974	H645	H947	H732	H1021
F-helix (C-lobe)	RS0	None	D774	D1062	D775	D1063	D735	D1036	D707	D1009	D796	D1083
R-shell												
Two residues upstream from the gatekeeper	Sh3	43	M664	L953	M665	L954	L624	L927	M598	L900	M685	L976
Gatekeeper, end of β5-strand	Sh2	45	E666	M955	E667	M956	Q626	M929	Q600	M902	T687	M978
αC-β4 loop	Sh1	36	V650	V937	V651	V938	V610	V911	V585	V884	A671	I960
Catalytic spine												
β2-strand (N-lobe)	CS8	15	I596	V888	I597	V889	I559	V863	I535	V863	V603	V911
β3-AxK-A (N-lobe)	CS7	11	I619	A905	I620	A906	L579	A880	L554	A853	V640	A928
β7-strand (C-lobe)	CS6	77	L720	L1009	L721	L1010	L680	L983	L654	L956	L741	L1030
β7-strand (C-lobe)	CS5	78	L721	V1010	L722	V1011	L681	V984	L655	V057	L742	L1031
β7-strand (C-lobe)	CS4	76	L719	V1008	L720	V1009	I679	I982	V653	I955	I740	V1029
D-helix (C-lobe)	CS3	53	L674	L963	L675	L964	L634	L937	I608	L910	L695	L986
F-helix (C-lobe)	CS2	None	T781	T1069	I782	T1070	T742	V1043	T714	S1012	T803	T1090
F-helix (C-lobe)	CS1	None	I785	L1073	I786	L1074	I746	L1047	V718	V1016	I807	L1094

[a]From Refs. [17,20,21], https://klifs.net/, and https://www.uniprot.org/uniprotkb/.

R-spine [22].

The protein kinase spine and shell residues perform a crucial role in the structure and activity of these enzymes; their importance in the operation of this enzyme family and their interactions with small molecule protein kinase inhibitors cannot be overemphasized. For an analysis of the characteristics of the spine and shell residues and their interactions with small molecule inhibitors of several members of the protein kinase superfamily, see the following articles: Refs. [23–25] for the ALK pleotrophin and midkine receptor protein-tyrosine kinase, Refs. [26–28] for the EGFR family of protein-tyrosine kinases, Ref. [29] for the PDGFRα/β protein-tyrosine kinases, Ref. [30] for the Kit stem cell receptor protein-tyrosine kinase, Ref. [31] for the VEGFR1/2/3 protein-tyrosine kinases, Ref. [32] for the fibroblast growth factor receptor family of protein-tyrosine kinases, Ref. [33] for the Flt3 receptor protein-tyrosine kinase; Ref. [34] for the RET glial-cell derived receptor protein-tyrosine kinase, Ref. [35] for the ROS1 orphan receptor protein-tyrosine kinase, Ref. [36] for the Bruton nonreceptor protein-tyrosine kinase, Refs. [37,38] for the Src nonreceptor protein-tyrosine kinase, Refs. [39,40] for the MEK1/2 dual specificity protein kinases, Refs. [41,42] for the cyclin-dependent protein-serine/threonine kinase family, Refs. [43,44] for the RAF protein-serine/threonine kinase, Refs. [45,46] for the ERK1/2 protein-serine/threonine kinases, Ref. [47] for phosphatidylinositol 3-kinase, a member of the atypical protein kinase family, and Ref. [48] for the Janus nonreceptor protein-tyrosine kinase family.

2.3. Regulation of Janus kinase activity

2.3.1. Role of the cytokine receptors

Dysregulation of protein kinases leads to many pathological conditions and it is therefore necessary that they are strictly regulated [10]. In contrast to general metabolic enzymes such as hexokinase, which catalyze the phosphorylation of thousands of molecules per minute, protein kinases mediate the phosphorylation of limited amounts of protein substrates. For example, when a Janus kinase is activated by its cytokine receptor, the main phosphorylated product is a Janus kinase that results from the trans-phosphorylation of one Janus kinase by another [48]. These enzymes also catalyze the phosphorylation of STATS and the cytokine receptors. The concentration of Janus kinases and their substrates are nearly equivalent and high turnover is unnecessary. The mechanisms for the interconversion of inactive and active protein kinases vary with the particular kinase and are generally quite intricate as seen for the Janus kinases.

Glassman et al. hypothesize that dormant JAK proteins exist in an autoinhibited monomeric form in which the protein-tyrosine kinases JH1 domain folds back on the FERM-SH2 domain resulting in the occlusion of the activation segment and the enzyme active site [49]. This closed state disallows JAK dimerization because of a steric clash between the pseudokinase domain and the FERM domain of a potential dimer partner. The closed state "breaths," however, to form a transient open state. Activation by cytokine-mediated receptor dimerization results in the formation of a JAK dimer and shifts the equilibrium from the autoinhibited state to the open state thereby promoting full activity of the JH1 kinase domain while concomitantly establishing the close proximity of apposing protein-tyrosine kinases to facilitate transphosphorylation.

Glassman et al. determined the structure of the entire active dimer of (murine) JAK1 using cryo-electron microscopy [49]. They used a mouse interferon lambda receptor (IFNλR) dimer construct artificially linked with a GCN4 leucine zipper to produce an intracellular receptor dimer. This receptor construct binds to JAK1 dimers and was even used in their purification. The authors describe the rationale for using this particular JAK1 construct, which has better expression and stability properties when compared with other JAKs. Note, however, that JAK1 forms only physiological heterodimers with other members of the JAK family owing to receptor-receptor interactions. Two important portions of the IFNλ receptor include a proline-containing box 1 segment (^{263}PRALDF^{268}) and hydrophobic box 2 segment (^{289}LIL^{291}), which are important JAK interacting components. Going from the N-terminus to the C-terminus of JAK1 are the FERM, SH2, the JH2 pseudokinase domain, and finally the JH1 protein-tyrosine kinase domains (Fig. 3).

The amino-terminal FERM and SH2 domains interact with the intracellular juxtamembrane segment of the paired INFλ receptor [49]. The FERM-SH2 components lie above the inward-facing pseudokinase domains that form a head-to-head dimer at the center of the complex. This interaction positions the carboxyterminal protein-tyrosine kinase (JH1) domain at the bottom of the JAK1 homodimer with their catalytic clefts and activation segments in an open configuration thereby poised for catalysis. The IFNλ receptor F285 backbone carbonyl hydrogen bonds with the JAK1 SH2 T532 side chain (not shown). The carbonyl part of the FERM-SH2 linker residue Y422 interacts with the ΨK R842 side chain. On the opposite side of the pseudokinase domain, the side chain of ΨK residue E800 forms a salt bridge with the side chain of R929 of the JH1 kinase domain and the side chain of ΨK R803 hydrogen bonds with the backbone carbonyl group of K940 in the β4-helix of JH1. As noted above, the pseudokinase domain of the Glassman construct has an inactive structure with αC-helix out and a closed activation segment. In contrast, the JH1 kinase domain has an active structure with αC_{in} and an open activation segment.

2.3.2. Aberrant regulation by JAK family mutations

JAK family gain of function mutations are associated with a diverse set of hematological disorders including B and T cell acute lymphoblastic leukemia (B-ALL, T-ALL), acute myeloid leukemia (AML), and

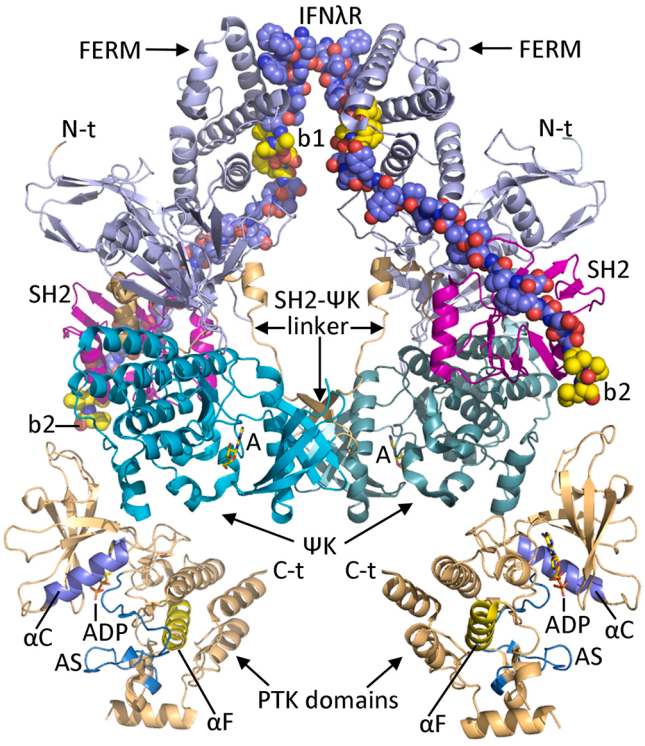

Fig. 3. Overview of the mouse JAK1 protein in complex with the mouse interferon lambda receptor (IFNλR). A portion of the IFNλ receptor is shown as spheres. b1 (box 1) and b2 (box 2) portions of IFNλR are shown with yellow carbon atoms. A refers to adenosine bound to the JAK1 pseudokinase (ΨK) or JH2 domain. AS is the activation segment of JH1. PTK, protein-tyrosine kinase or the JH1 domain. N-t and C-t are the amino-terminal and carboxyterminal ends of JAK1. Going from the N-terminus to the C-terminus of JAK1, FERM is colored light blue, SH2 is magenta, the pseudokinase is cyan, and the protein-tyrosine kinase is tan with a dark blue αC-helix, blue activation segment, and yellow αF-helix. The PDB ID is 7t6f.

myeloproliferative neoplasms (MPN) as outlined in Table 4. The inhibitory JH2-JH1 interaction interface harbors most of the known clinical activating JAK mutations and disruption of this inhibitory interaction represents one mechanism accounting for an activated phenotype. Myeloproliferative neoplasms include polycythemia vera, myelofibrosis, and essential thrombocythemia [51]. An activating JAK2 V617F mutation occurs in about 95% of people with polycythemia vera and in about 50% of cases of myelofibrosis and essential thrombocythemia. Glassman et al. suggest that the mechanism of V617F JAK2 activation is a result of the increased hydrophobic interaction of the mutant phenylalanine compared with the wildtype valine with its partner dimer [49].

Several *JAK2* mutations in the SH2-pseudokinase linker – exon 12 (^{535}MVFHKIRNEDLIF^{547}) – lead to polycythemia vera while mutations within the N-lobe of the JH2 pseudokinase domain lead to ALL and polycythemia vera [52]. Many JAK2 mutations in lymphoid lineage neoplasms involve R683; this residue occurs at the end of the β7'-strand beneath the site corresponding to the position where the adenine base of JH2 binds; this site has the potential to interact with the β2–β3 loop of the small lobe of JH1. Mutations of the *JAK3* pseudokinase small lobe are found in acute megakaryoblastic leukemia (15%) while carboxyterminal lobe mutations are found in ALL. *TYK2* mutations have been described in about 20% of people with T-ALL [53]. In contrast to enzyme activation, TYK2 deficiencies are associated with susceptibility to bacterial and viral infections and several *TYK2* polymorphisms demonstrate a strong linkage to autoimmune illnesses such as Crohn disease, systemic lupus erythematosus, multiple sclerosis, primary biliary cirrhosis, and type I diabetes. Furthermore, *TYK2* polymorphisms have also been linked to AML.

Table 4
Selected JAK family mutations and neoplastic diseases[a,b].

Exon	Mutation	Location	Disease
JAK1			
6	K204M	FERM	B-ALL
10	T478S	SH2	AML
11	S512L	SH2	T-ALL
13	V623A	ΨK	AML
14	A634D	ΨK	B-All, T-ALL
14	S646P/F	ΨK	ALL
14	V658F/L	ΨK	ALL
16	R724H/Q	ΨK	B-All, T-ALL
19	R879S/C/H/S	ΨK	T-ALL
JAK2			
12	K539L	SH2-ΨK linker	MPNs
14	L611S	ΨK	ALL
14	V617F	ΨK	MPNs
16	R683G/S	ΨK	MPNs
20	R867Q	PTK	ALL & hereditary thrombocythemia
20	D873N	PTK	ALL
20	T875N	PTK	AMKL
21	P933R	PTK	ALL
25	N1108S	PTK	PV
JAK3			
4	P132T/A	FERM	AMKL
11	M511I	SH2-ΨK linker	AML, T-PLL, JMML, NKTCL
13	A572V/T	ΨK	AMKL
13	A573V	ΨK	DS-ALL, DS AMKL, NKTCL
16	V722I	ΨK	AMKL, SCID, NKTCL
TYK2			
15	R703W	ΨK	AML
20	A928V	PTK	ALL
20	E957D	PTK	AML
22	R1027H	PTK	ALL

[a]Data from Ref. [50].
[b]ALL, Acute lymphoblastic leukemia; AML, Acute myeloid leukemia; AMKL, Acute megakaryoblastic leukemia; B-ALL, B-cell acute lypmphoblastic leukemia; DS- Down syndrome; JMML, Juvenile myelomonocytic leukemia; MPN, myeloproliferative neoplasm; NKTCL, NK/T-cell lymphoma; PTK, protein-tyrosine kinase; PV, polycythemia vera; ΨK, JH2 pseudokinase domain; SCID, severe combined immunodeficiency; T-ALL, T-cell acute lymphoblastic leukemia; T-PLL, T-cell prolymphocytic leukemia.

Rare chromosomal rearrangements linking the JH1 domain-coding portion of the *JAK2* gene to the oligomerization domain of either BCR, TEL, Pax5, PCM1, or ETV6 have been reported in atypical chronic myelogenous leukemia [53]. The fusion proteins form oligomers and promote the transphosphorylation of their partner activation segments that result in JAK2 JH1 activation and subsequent downstream signaling including the STAT, MAP kinase, or phosphatidylinositol-3 kinase pathways. Furthermore, the *JAK2* locus is amplified in 30–50% of Hodgkin lymphomas and in some B-cell lymphomas. Increased JAK-STAT signaling has also been implicated in the pathogenesis of various solid tumors including breast, esophageal, gastric, ovarian, and lung, head and neck squamous cell cancers, and melanoma [54].

3. Protein kinase-inhibitor classification and inhibitor binding pockets

Based upon previous work [55–58], we divided the small molecule protein kinase blockers into seven main groups including reversible (Groups I, I½, II, III, IV, and V) and irreversible inhibitors (VI) (Table 5). Type I and I½ inhibitors have the DFG-D_{in} conformation and the type II inhibitors have the DFG-D_{out} conformation. We split the type I½ and type II inhibitors into A and B subtypes [22]. Subtype A drugs are those that extend past the gatekeeper residue into the back cleft while subtype B drugs do not extend into the back cleft. The possible significance of this difference, based on incomplete data, is that subtype A inhibitors bind to their enzyme target with longer residence times when compared with subtype B inhibitors. For example, sorafenib is a type IIA and sunitinib is a type IIB inhibitor of VEGFR, both drugs of which are FDA-approved for the treatment of renal cell carcinoma. The type IIA antagonist has a residence time greater than 64 min while the type IIB inhibitor has a residence time less than 2.9 min [22].

Modi and Dunbrack performed a comprehensive analysis of the interactions of drugs and ligands with functional and dormant conformations of protein kinases based upon the structure of the activation segment, which begins with the DFG signature [60]. These investigators formulated a grouping of protein kinase conformations based upon the position of the phenylalanine side chain (DFG-D_{in}, DFG-D_{out}, and DFG-D_{inter} or intermediate) and the backbone dihedral angles of the xDF arrangement, where x is the residue before DFG. They identified eight different configurations and identified them based on the Ramachandran regions (A, alpha; B, beta; L, left) of the xDF motif and the χ1 phenylalanine rotamer (minus, plus, trans). Their clustering protocol divides the DFG-D_{in} conformation into six clusters including BLAminus, which contains active structures, and two common dormant forms – BLBplus and ABAminus. DFG_{out} structures are predominantly in the BBAminus group. The inactive structures have features that disallow their binding to ATP, Mg^{2+}, and/or their protein substrates. These investigators created a valuable and noncommercial web site

Table 5
Classification of small molecule protein kinase inhibitors[a].

Inhibitor type	Properties
I	Binds in and around the ATP-binding pocket of an active enzyme
I½ A/B	Binds in and around the ATP-binding pocket of an inactive DFG-D_{in} enzyme
I½ A	Extends into the back cleft
I½ B	Does not extend into the back cleft
II A/B	Bind in and around the ATP-binding site of an inactive DFG-D_{out} enzyme
II A	Extends into the back cleft
II B	Does not extend into the back cleft
III	Allosteric inhibitor bound next to the ATP-binding site
IV	Allosteric inhibitor bound away from the ATP-binding site
V	Bivalent inhibitor spanning two kinase domain regions
VI	Covalent inhibitor

[a] Adapted from Ref. [59].

(http://dunbrack3.fccc.edu/kincore/) that enables one to determine whether the protein kinase conformations correspond to a functional enzyme (DFG-D_{in}, BLAminus) or a dormant enzyme (otherwise). We used this web site to ascertain if the structure of the various protein kinases of the drug-enzyme complexes that we are considering are active (DFG-D_{in}, BLAminus) or inactive.

We followed the lead of Liao [61], van Linden et al. [62], and Kanev et al. [63] in describing protein kinase drug-binding pockets. A summary portraying the locations of the drug-binding pockets and subpockets is provided in Table 6 and Fig. 4 [62]. These authors divided the region between the protein kinase amino-terminal and carboxyterminal lobes into a front pocket or front cleft, a gate area, and a back cleft. Hydrophobic pocket II (HPII) or the back pocket is made up of the gate area and back cleft. The front cleft includes the glycine-rich loop, the adenine-binding pocket, the hinge residues, the linker segment connecting the hinge residues to the large lobe αD-helix, and the catalytic loop (HRD(x)$_4$N) (Table 7). The gate area includes the β3-strand of the small lobe and the DFG of the activation segment. The back-cleft extends to the αC-β4 back loop, to portions of the β4- and β5-strands of the small lobe, to the αC-helix, and to a section of the αE-helix within the large lobe.

van Linden et al. and Kanev et al. produced a complete listing of drug and ligand binding interaction sites that includes more than 6000 human and mouse protein kinase domains [62,63]. Their KLIFS (kinase–ligand interaction fingerprint and structure) catalogue includes an alignment of 85 ligand binding-site residues occurring in both small and large lobes; this catalogue facilitates the classification of drugs and ligands depending upon their binding properties that assist in the detection of common and unique interactions. Moreover, these investigators devised a standard amino acid residue numbering system that allows for the comparison of various protein kinases. Fig. 5 depicts the location of the KLIFS residues within the protein kinase domain and Table 3 lists the relationship of the KLIFS database nomenclature and the catalytic spine, shell, and regulatory spine amino acid residue numbering system. Furthermore, these scientists established a useful free and searchable web site that is regularly updated thereby providing complete data on the interactions of protein kinases with drugs and ligands (https://klifs.net/).

Additionally, Carles et al. created a comprehensive listing of therapeutic protein kinase inhibitors that have been approved by various international agencies or that are in clinical trials [64]. They have established a noncommercial and searchable web site that is regularly updated that depicts the inhibitor structures, physical properties, therapeutic indications, year of first approval (if applicable), trade name, and their protein kinase targets (http://www.icoa.fr/pkidb/). The Blue Ridge Institute for Medical Research maintains a web site that lists the FDA-approved protein kinase blockers and provides their (i) structures, (ii) number of hydrogen bond donors/acceptors, (iii) calculated log of the distribution coefficient, (iv) number of rotatable bonds and rings, (v) year of initial approval, (vi) presumed protein kinase targets, (vii) clinical indications, and (viii) links to their FDA labels. This web site, which is regularly updated, is found at www.brimr.org/PKI/PKIs.htm.

Table 6
Location of KLIFS sub-pockets[a].

Sub-pocket	KLIFS residues[b]	Description[c]
FP-I	75, 79–82	Between DFG and HRD(x)$_4$N-N of the CL of DFG-$D_{in/out}$
FP-II	4–10	Near the open GRL conformation of DFG-$D_{in/out}$
BP-I-A	16–17, 43–45	Found in the upper gate area against/between the β-3 and β-5 sheets of DFG-$D_{in/out}$
BP-I-B	16–17, 28, 43,81– 82	Between DFG and the β-3 and β-5 sheets of DFG-$D_{in/out}$
BP-II-in	24, 28, 35–38, 82	Between DFG, the αC-helix, and the back loop of DFG-D_{in}
BP-II-A-in	28, 35–38, 82	Between DFG, the back loop, and the β-4 sheet of DFG-D_{in}
BP-II-B	24, 28, 38, 82	Near DFG-F, αC-E, and the proximal β-4 strand of DFG-$D_{in/out}$
BP-II-out	27, 31, 35, 61, 66, 68	Near the distal αC-helix, the back loop, and above the HRD-H of DFG-D_{out}
BP-III	31, 35, 79	Near the back loop and DFG-D minus 2 of DFG-D_{out}
BP-IV	27, 66–68	Deep in the back pocket near the distal αC-helix and HRD of DFG-D_{out}
BP-V	20, 23, 24, 27	Beneath αC-E and the middle of the αC-helix of DFG-D_{out}

[a] Curated data provided by Dr. Albert J. Kooistra.
[b] klifs.net.
[c] CL, catalytic loop; GRL, glycine-rich loop.

4. FDA-approved Janus kinase inhibitors

4.1. Survey of therapeutic JAK-family antagonists

The seven JAK-family inhibitors that are FDA-approved for human use are listed in Table 8 along with their therapeutic indications and targets. These drugs are used for the treatment of both inflammatory and neoplastic disorders. Abrocitinib, ruxolitinib, and upadacitinib are approved for the treatment of atopic dermatitis whereas baricitinib is used for the treatment of rheumatoid arthritis and covid 19. Tofacitinib and upadacitinib are JAK antagonists that are used for the treatment of rheumatoid arthritis and ulcerative colitis. Additionally, ruxolitinib is approved for the treatment of polycythemia vera; fedratinib, pacritinib, and ruxolitinib are approved for the treatment of myelofibrosis. A few other FDA-approved indications are listed in Table 8. Abrocitinib and upadacitinib target JAK1. In contrast, fedratinib targets JAK2 and JAK3 while pacritinib blocks the activity of JAK2. With low nanomolar inhibitory constants, ruxolitinib and tofacitinib are pan-JAK family inhibitors while baricitinib blocks the activity of JAK1, JAK2, and TYK2 (Table 9).

4.2. Abrocitinib-JAK1/2 complexes

Abrocitinib is a pyrrolopyrimidine derivative (Fig. 6A) that is approved for the treatment of atopic dermatitis (Table 8). It is a potent JAK1 antagonist with moderate activity against JAK2 (Table 9). Vazqeez et al. determined the X-ray structure of this drug bound to JAK1 and they demonstrated that the pyrrolo N–H hydrogen bonds with the backbone carbonyl oxygen of E957 (the first hinge residue) and the pyrimidine N1 hydrogen bonds with the N–H backbone of L959 (the third hinge residue) [82]. Furthermore, the drug amino N–H hydrogen bonds with the side chain carbonyl moiety of the catalytic loop asparagine (N1008) and a drug sulfonamide oxygen hydrogen bonds with the N–H of the side chain of R1007 of the catalytic loop (Fig. 7A). The pyrimidine N3 forms a hydrogen bond with a water molecule that in turn hydrogen bonds with E966 within the αD-helix. The comparable residue in JAK2 is the shorter aspartate so that this water-mediated hydrogen bond is unable to form. This accounts in part for the greater affinity of abrocitinib for JAK1 than for JAK2 [82]. The drug makes hydrophobic contact with the first two shell residues, three catalytic spine residues (CS6/7/8) and KLIFS residues 3, 80, and 81 (Table 10). The KLIFS-3 residue occurs immediately before the G-rich loop, KLIFS-80 is the x residue of xDFG, and KLIFS-81 is the DFG-D residue. The drug also interacts hydrophobically with ^{882}GEG^{884} and G887 of the glycine-rich loop, AxK-K908 of the β3-strand, and residues F958, L959, G962, and S963 of the hinge-linker segment. The drug occupies the front pocket and FP-I/II of an active DFG-D_{in} enzyme and it is classified as a type I inhibitor [22]. See Ref. [83] for information on the clinical trials that led to the approval of abrocitinib in 2022.

Vazquez et al. determined the X-ray structure of abrocitinib bound to JAK2 [82] and found that its interactions mirrored its binding to JAK1. These investigators found that the pyrrolo N–H hydrogen bonds with the backbone carbonyl group of E930 (the first hinge residue) and the

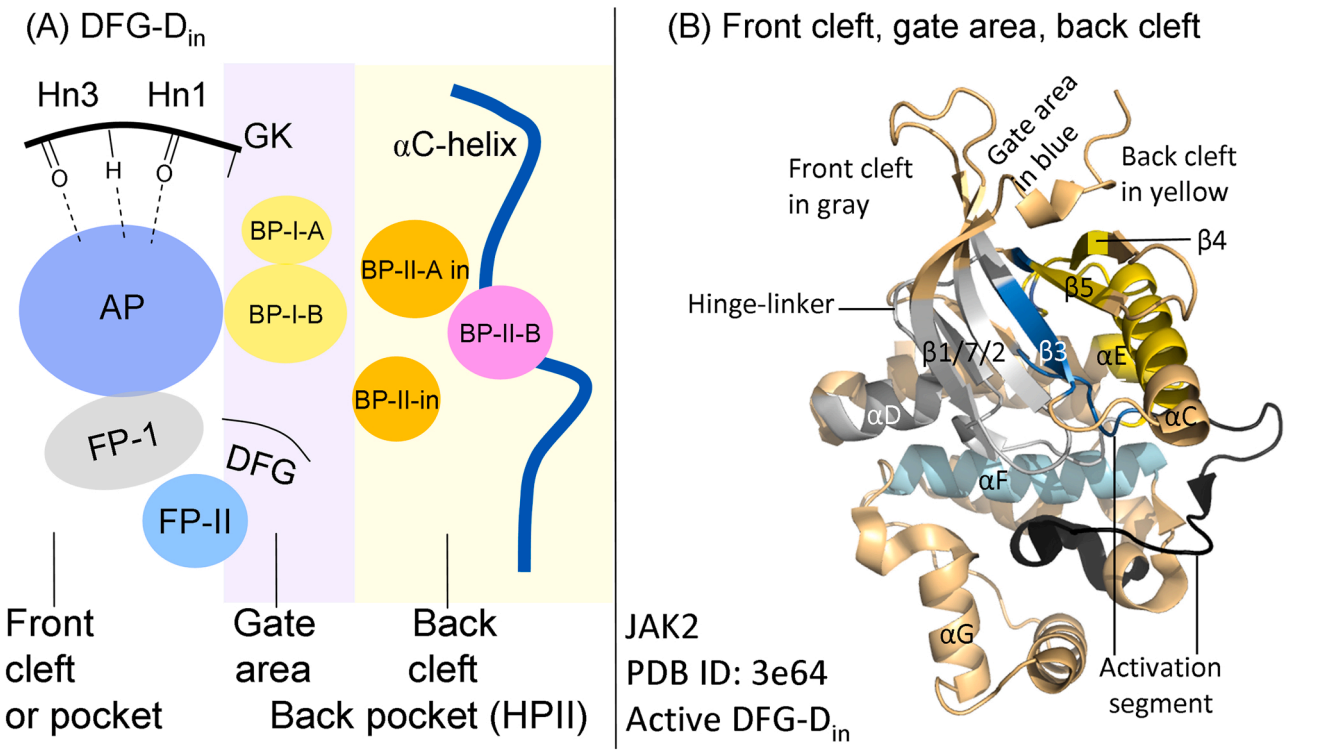

Fig. 4. (A) Sketch of the binding pockets of the active DFG-D_{in} protein-kinase conformation. (B) Location of the front cleft, gate area, and back cleft of the active human JAK2 JH1 domain. AP, adenine-binding pocket; FP, front pocket; BP, back pocket; GK, gatekeeper; Hn, hinge.

Table 7
Location of selected catalytic cleft residues[a].

Description	Location	KLIFS residue no.
GxGxΦG	Front cleft	4–9
β2-strand V (CS7)	Front cleft	11
β3-strand A (CS8)	Front cleft	15
β3-strand AxK-K	Front cleft	17
Catalytic loop: HRD(x)$_4$N	Front cleft	68–75
HRD with DFG-D_{in}	Front cleft	68–70
HRD(x)$_4$N-N	Front cleft	75
β7-strand CS6	Front cleft	77
αC-β4 back loop residue	Gate area	36
Gatekeeper	Gate area	45
Hinge	Gate area	45–47
Linker	Gate area	48–52
x of xDFG	Gate area	80
DFG	Gate area	81–83
αC-helix E	Back cleft	24
RS3	Back cleft	28

[a] Curated data provided by Dr. Albert J. Kooistra; klifs.net.

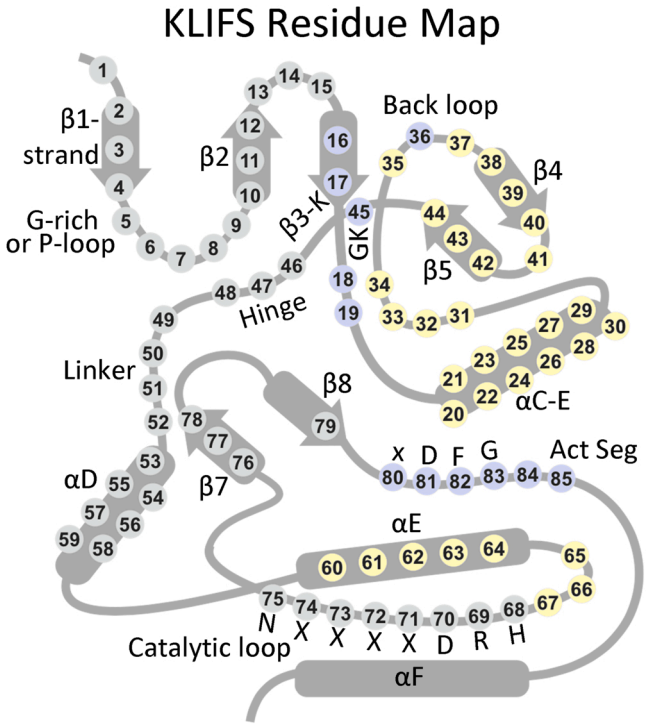

Fig. 5. Standard KLIFS residue numbers and their location within the protein kinase domain. Gray residues reside within the front cleft; blue residues, gate area; yellow residues, back cleft. Act Seg, activation segment; GK, gatekeeper.

pyrimidine N1 hydrogen bonds with the N–H backbone of L932. Moreover, the N–H of the drug hydrogen bonds with the side chain carbonyl portion of the catalytic loop asparagine (N981) and a drug sulfonamide oxygen hydrogen bonds with the N–H of the terminal side chain of R980 of the catalytic loop (Fig. 7B). The drug makes hydrophobic contact with the first two shell residues, three catalytic spine residues (CS6/7/8) and KLIFS residues 3, 80, and 81 (Table 10). The drug also interacts hydrophobically with ^{856}GEG^{858} and G861 of the glycine-rich loop, AxK-K882 of the β3-strand, along with residues Y931, L932, G935, and S936 of the hinge-linker segment. The N3 of abrocitinib hydrogen bonds with a water molecule in the JAK2-drug complex, and this water molecule is 5.9 Å from the side chain of D939 within the αD-helix – too long to form a hydrogen bond. In contrast, the distance from the water in the JAK1-abrocitinib structure is 3.3 Å from the analogous E966 – which is within hydrogen bonding distance. This difference explains in part the greater affinity of abrocitinib for JAK1 than for JAK2 [82]. The drug occupies the front pocket and FP-I/II of an active DFG-D_{in} enzyme and it is grouped with other type I inhibitors [22].

Table 8
FDA-approved JAK family inhibitors and indications[a].

Drugs	Targets	Diseases	Approval date	Clinical trials	Refs.
Abrocitinib	JAK1, JAK2	Atopic dermatitis	2022	NCT03627767 NCT03720470	[65]
Baricitinib	JAK1, JAK2, TYK2	Rheumatoid arthritis	2018	NCT02265705 NCT01710358	[66, 67]
		Covid 19	2022	NCT04421027 NCT04401579	[68]
Fedratinib	JAK2, JAK2 V617F, JAK3	Myelofibrosis	2019	NCT00724334 NCT00631462 NCT01437787	[69]
Pacritinib	JAK2, JAK2 V617F	Myelofibrosis	2022	NCT04884191	[70]
Ruxolitinib	JAK1, JAK2, JAK2 V617F, JAK3, TYK2	Myelofibrosis	2011	NCT00952289	[71]
		Polycythemia vera	2014	NCT02038036	[72]
		Acute and chronic graft vs. host disease	2019, 2021	NCT03112603 NCT03147742	[73]
Tofacitinib	JAK1, JAK2, JAK3, TYK2	Rheumatoid arthritis	2012	NCT02187055	[66]
		Psoriatic arthritis	2017	NCT01877668	[74]
		Ulcerative colitis	2018	NCT03281304	[74]
		Juvenile idiopathic arthritis	2020	NCT02592434	[75]
		Ankylosing spondylitis	2021	NCT03502616	[76]
Upadacitinib	JAK1	Rheumatoid arthritis	2019	NCT02706847	[77]
		Psoriatic arthritis	2021	NCT03104400	[78]
		Atopic dermatitis	2022	NCT03738397	[79]
		Ulcerative colitis	2022	NCT02819635	[80]

[a] Data from Ref. [81].

Table 9
Janus kinase inhibitor EC_{50} values (nM)[a,b].

Drug	JAK1	JAK2	JAK3	TYK2
Abrocitinib	5.01	39.8	501	1260
Baricitinib	1.00	0.79	25.1	7.94
Fedratinib	100	3.16	1.00	20.0
Pacritinib	1280	23	520	50
Ruxolitinib	0.079	0.039	2.51	0.40
Tofacitinib	0.50	0.50	0.16	3.98
Upadacitinib	43	120	2300	4700

[a] EC_{50} (effective concentration) refers to IC_{50}, K_d, or K_i.
[b] Ref. [81].

4.3. Baricitinib-JAK2 interactions

Baricitinib is a pyrrolopyrimidine derivative (Fig. 6B) that is approved for the treatment of rheumatoid arthritis and hospitalized covid 19 patients aged two to 18 years (Table 8). This agent is a potent inhibitor of JAK1 and JAK2 and a modest TYK2 antagonist (Table 9). Chang et al. determined the X-ray structure of this drug bound to JAK2 and they demonstrated that the pyrrolo N–H hydrogen bonds with the backbone carbonyl oxygen of E930 (the first hinge residue) and the pyrimidine N1 hydrogen bonds with the N–H backbone of L932 (Fig. 7B) [84]. The drug makes hydrophobic contact with the first two shell residues, three catalytic spine residues (CS6/7/8) and KLIFS residues 3, 80, and 81 (Table 10). The drug also interacts hydrophobically with G858 and G861 of the glycine-rich loop, S862 of the β3-strand, Y931 and L932 of the hinge-linker segment, and R980 and N981 of the catalytic loop. The medicine is found in the front pocket and FP-I/II of an active DFG-D_{in} enzyme and it is considered to be a type I inhibitor [22]. See Refs. [74,81,83,85] for information on the clinical trials that supported the approval of baricitinib for the treatment of rheumatoid arthritis in 2018 and covid 19 in 2022.

4.4. Fedratinib-JAK2 interactions

Fedratinib is an anilino-pyrimidine derivative (Fig. 6C) that is approved for the treatment of myelofibrosis (Table 8). This agent is a potent inhibitor of wildtype JAK2, the V617F JAK2 mutant, and JAK3 (Table 9). Davis et al. determined the X-ray structure of this drug bound to JAK2 and they demonstrated that the pyrimidine N1 hydrogen bonds with the N–H backbone of L932 and the anilino N–H hydrogen bonds with the carbonyl portion of this same third hinge residue (Fig. 7D) [86]. The drug makes hydrophobic contact with the gatekeeper residue (Sh2), three catalytic spine residues (CS6/7/8) and KLIFS residues 3 and 81 (Table 10). The drug also interacts hydrophobically with ^{853}QQLGKG^{858} of the β1-strand and the glycine-rich loop, S862 of the β2 strand, AxK-K882 of the β3-strand, plus ^{930}EYLP^{933} and G935 of the hinge-linker segment. The compound is found in the front pocket and FP-II of an active DFG-D_{in} enzyme and we classified it as a type I antagonist [22]. See Refs. [74,81] for data on the clinical trials that led to the approval of fedratinib in 2019.

4.5. Ruxolitinib-JAK2 interactions

Ruxolitinib is a is a pyrrolopyrimidine derivative (Fig. 6E) that is approved for the treatment of myelofibrosis, polycythemia vera, and acute and chronic graft vs. host disease (Table 8). It is a potent JAK1 and JAK2 antagonist with moderate activity against TYK2 (Table 9). Davis et al. determined the X-ray structure of this medicinal agent bound to JAK2 and they demonstrated that the pyrrolo N–H hydrogen bonds with the backbone carbonyl oxygen of E930 (the first hinge residue) and the pyrimidine N1 hydrogen bonds with the N–H backbone of L932 (Fig. 7E) [86]. The drug makes hydrophobic contact with the first two shell residues, three catalytic spine residues (CS6/7/8) and KLIFS residues 3, 80, and 81 (Table 10). The drug also interacts hydrophobically with ^{856}GKG^{858} and ^{861}GSV^{863} of the glycine-rich loop and the β2-strand, AxK-K882 of the β3-strand, Y931 and L932 of the hinge, and residues R980 and N981 of the catalytic loop. Ruxolitinib occupies the front pocket and FP-I/II of an active DFG-D_{in} enzyme and it is grouped with type I inhibitors [22]. See Refs. [74,81] for information on the clinical trials that supported the approval of ruxolitinib in 2011.

4.6. Tofacitinib-JAK family interactions

Tofacitinib is a is a pyrrolopyrimidine derivative (Fig. 6F) that is approved for the treatment of rheumatoid, psoriatic, and idiopathic juvenile arthritis, ulcerative colitis, and ankylosing spondylitis (Table 8). It is a potent JAK family inhibitor (a pan-inhibitor) with low nanomolar IC_{50} values against JAK1/2/3 and TYK2 (Table 9). Williams et al. determined the X-ray structure of this drug bound to JAK1 and they demonstrated that the pyrrolo N–H hydrogen bonds with the backbone carbonyl oxygen of E957 (the first hinge residue) and the pyrimidine N1 hydrogen bonds with the N–H backbone of L959 (Fig. 7F) [87]. The drug makes hydrophobic contact with the first two shell residues, three catalytic spine residues (CS6/7/8) and KLIFS residues 3, 80, and 81 (Table 10). The drug also interacts hydrophobically with ^{882}GEG^{884} and G887 of the G-rich loop, AxK-K908 of the β3-strand, plus F958, L959, G962, and S963 of the hinge-linker segment. The drug occupies the front pocket and FP-I/II of an active DFG-D_{in} enzyme and it is considered to be a type I inhibitor [22]. See Refs. [74,81] for information on the clinical trials that supported the approval of tofacitinib.

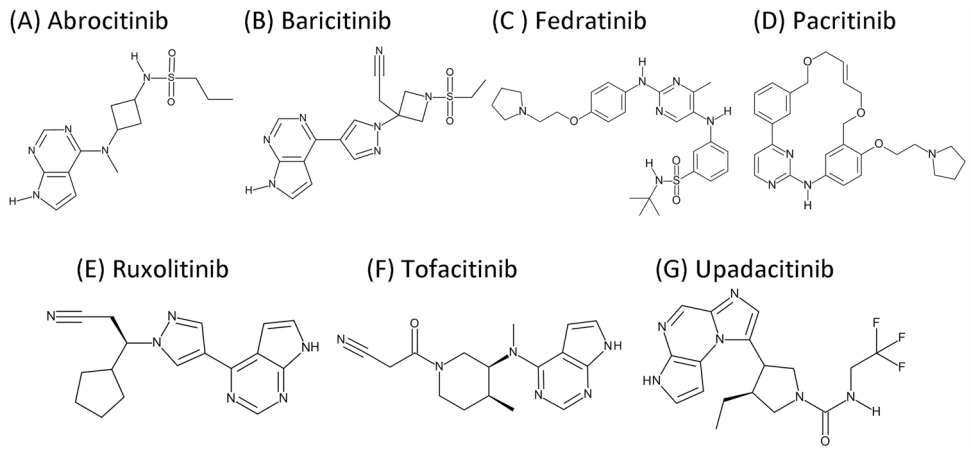

Fig. 6. Structures of FDA-approved human therapeutic JAK-family kinase antagonists.

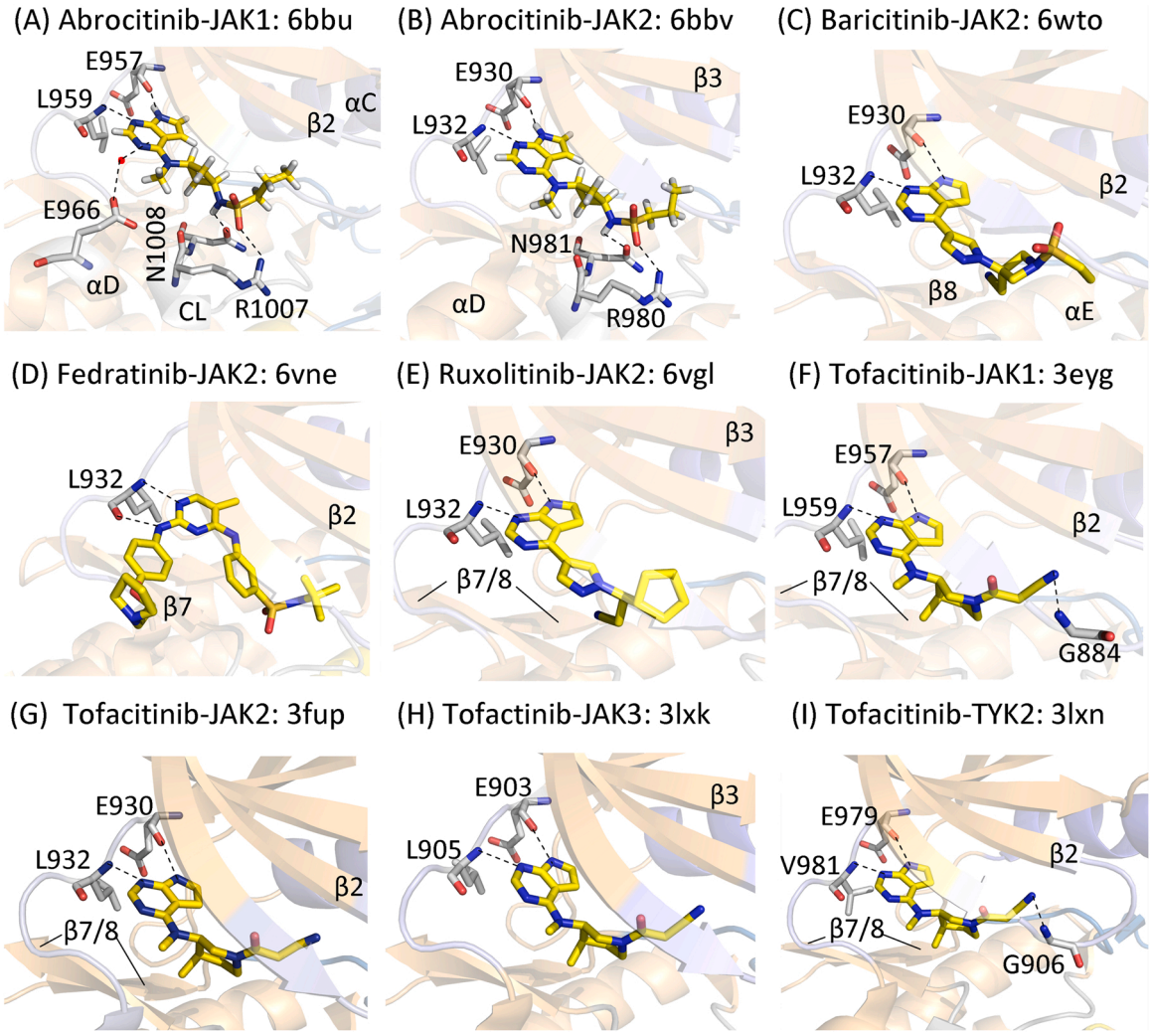

Fig. 7. JAK kinase-drug complexes. The PDB ID numbers are provided with each complex. CL, catalytic loop. Dashes represent polar bonds. The carbon atoms of the drug are colored yellow and those of the protein are gray.

Williams et al. determined the X-ray structure of tofacitinib bound to JAK2 and they demonstrated that the pyrrolo N–H hydrogen bonds with the backbone carbonyl moiety of the first hinge residue (E957) and the pyrimidine N1 hydrogen bonds with the N–H backbone of L932 (Fig. 7G) [87]. The drug makes hydrophobic contact with the first two shell residues, three catalytic spine residues (CS6/7/8) and KLIFS residues 3, 80, and 81 (Table 10). The drug also interacts hydrophobically with ^{856}GKG^{858} and G861 of the G-rich loop, AxK-K882 of the β3-strand, residues Y931, L932, G935, and S936 of the hinge-linker segment, residue N981 at the end of the catalytic loop, and I982 and L983 of the

Table 10
Human drug-enzyme hydrophobic (Φ) interactions using their designated KLIFS residue numbers[a].

	PDB ID	Inhibitor type	Sh1	Sh2	Sh3	CS6	CS7	CS8	KLIFS			KLIFS pockets[b] & subpockets
KLIFS no. → Drug-enzyme ↓			36	45	43	77	11	15	3	80	81	
Abrocitinib-JAK1	6bbu	I	Φ	Φ	–	Φ	Φ	Φ	Φ	Φ	Φ	F, FP-I/II
Abrocitinib-JAK2	6bbv	I	Φ	Φ	–	Φ	Φ	Φ	Φ	Φ	Φ	F, FP-I/II
Baricitinib-JAK2	6wto	I	Φ	Φ	–	Φ	Φ	Φ	Φ	Φ	Φ	F, FP-I/II
Fedratinib-JAK2	6vne	I	–	Φ	–	Φ	Φ	Φ	Φ	–	Φ	F, FP-II
Ruxolitinb-JAK2	6vgl	I	Φ	Φ	–	Φ	Φ	Φ	Φ	Φ	Φ	F, FP-I/II
Tofacitinib-JAK1	3eyg	I	Φ	Φ	–	Φ	Φ	Φ	Φ	Φ	Φ	F, FP-I/II
Tofacitinib-JAK2	3fup	I	Φ	Φ	–	Φ	Φ	Φ	Φ	Φ	Φ	F, FP-I/II
Tofacitinib-JAK3	3lxk	I	Φ	Φ	–	Φ	Φ	Φ	Φ	Φ	Φ	F, FP-I/II
Tofacitinib-TYK2	3lxn	I	Φ	Φ	–	Φ	Φ	Φ	Φ	Φ	Φ	F, FP-I/II

[a] KLIFS-3, kinase-ligand interaction fingerprint and structure residue-3; from http://klifs.vu-compmedchem.nl/
[b] F, front pocket; Refs. [62,63].

β7-strand. The drug occupies the front pocket and FP-I/II of an active DFG-D_{in} enzyme and it is classified as a type I inhibitor [22].

Chrencik et al. determined the X-ray structure of tofacitinib bound to JAK3 and they demonstrated that the pyrrolo N–H hydrogen bonds with the backbone carbonyl oxygen of the first hinge residue (E903) and the pyrimidine N1 hydrogen bonds with the N–H backbone of L905 (Fig. 7H) [88]. The drug makes hydrophobic contact with the first two shell residues, three catalytic spine residues (CS6/7/8) and KLIFS residues 3, 80, and 81 (Table 10). The drug also interacts hydrophobically with ^{829}GKG^{831} of the G-rich loop, S835 and V836 of the β2-strand, AxK-K855 of the β3-strand, residues Y904 and L905 of the hinge segment, residue N954 at the end of the catalytic loop, and I955 and L956 of the β7-strand. The drug occupies the front pocket and FP-I/II of an active DFG-D_{in} enzyme and it is considered to be a type I inhibitor [22].

Chrencik et al. determined the X-ray structure of tofacitinib bound to TYK2 and they demonstrated that the pyrrolo N–H hydrogen bonds with the backbone carbonyl portion of the first hinge residue (E979) and the pyrimidine N1 hydrogen bonds with the N–H backbone of V981, and the nitrile hydrogen bonds with the N–H component of G906 (Fig. 7I) [88]. The drug makes hydrophobic contact with the first two shell residues, three catalytic spine residues (CS6/7/8), and KLIFS residues 3, 80, and 81 (Table 10). The drug also interacts hydrophobically with ^{904}GEG^{906} of the G-rich loop, AxK-K930 of the β3-strand, residues Y980, V981, and S985 of the hinge-linker segment, plus R1027 and N1028 at the end of the catalytic loop. The drug occupies the front pocket and FP-I/II of an active DFG-D_{in} enzyme and it is grouped with type I inhibitors [22].

4.7. Summary of the structures of the JAK family kinase-inhibitor complexes

All of the above JAK family kinase blockers are orally bioavailable and are classified as type I inhibitors as the enzyme conformation of the drug-protein complex corresponds to an active state [22]. Although there are some differences in the Fox Chase Cancer Center and the Blue Ridge Institute inhibitor classification schemes [89], Modi and Dunbrack determined that the JAK family inhibitor complexes described herein are included within their ABAminus cluster and they also classified them as type I antagonists [60]. The JH1 portion of the JAK kinases prefers to assume an active conformation even in the absence of activation segment phosphorylation. Each of the inhibitors described above occupy the front pocket and they do not extend to the gate area or the back pocket. All of them except fedratinib occupy the front pocket and FP-I/II and interact with Sh1, Sh2, CS6/7/8, and KLIFS residues 3, 80, and 81. Fedratinib occupies the front pocket, FP-II (not FP-I), interacts with Sh2 (not Sh1), and interacts with KLIFS residues 3 and 81 (and not 80). All of them except fedratinib form hydrogen bonds with the first and third hinge residues; fedratinib interacts with only the third hinge residue.

5. Physicochemical properties of orally effective drugs

5.1. Lipinski's rule of five (Ro5)

Pharmacologists and medicinal chemists have searched for the physicochemical properties of drugs that result in medicinal agents that are orally effective. Lipinski's rule of five (Ro5) is a computational and experimental procedure that is used to characterize efficacy, membrane permeability, and solubility in the drug-development setting [90]. It is a procedure that determines whether an agent with specific pharmacological properties may be orally effective. The Lipinski criteria were based on data showing that most orally bioavailable agents are relatively small and moderately lipophilic compounds. The Ro5 criteria are used during drug development and discovery as pharmacologically active lead compounds are sequentially optimized to increase their activity while retaining selectivity.

The Ro5 posits that reliable oral bioavailability is more likely to result when (i) the atom-based calculated Log P (ALogP) is 5 or less, when (ii) there are 5 or fewer hydrogen-bond donors, when (iii) there are 10 (5 × 2) or fewer hydrogen-bond acceptors, and when (iv) the molecular weight is 500 (5 × 100) or less [90]. The partition coefficient (P) is the ratio of the solubility of the nonionized agent in the organic phase of water-saturated *n*-octanol divided by its solubility in the aqueous phase. The P value reflects the hydrophobicity of the drug or ligand; the higher the P value, the greater the hydrophobicity. The sum of hydrogen-bond donors is the number of NH and OH groups. The sum of hydrogen-bond acceptors consists of the number of neutral heteroatoms minus heteroaromatic oxygen and sulfur atoms, pyrrole nitrogen atoms, halogen atoms, and higher oxidation states of sulfur, phosphorous, and nitrogen, but it does include the oxygen atoms bonded to them. The Ro5 is based on the physicochemical properties of more than two thousand reference drugs [90]. The seven approved JAK-family

Table 11
Properties of FDA-approved JAK family kinase inhibitors.

Drug	PubChem CID	Formula	MW (Da)	HD[a]	HA[b]	ALogP[c]
Abrocitinib	78323835	$C_{14}H_{21}N_5O_2S$	323	2	3	1.3
Baricitinib	44205240	$C_{16}H_{17}N_7O_2S$	371	1	7	1.1
Fedratinib	16722836	$C_{27}H_{36}N_6O_3S$	525	3	9	4.8
Pacritinib	46216796	$C_{28}H_{32}N_4O_3$	473	1	7	4.1
Ruxolitinib	25126798	$C_{17}H_{18}N_6$	306	1	4	3.5
Tofacitinib	9926791	$C_{16}H_{20}N_6O$	312	1	5	1.5
Upadacitinib	58557659	$C_{17}H_{19}F_3N_6O$	380	2	6	2.9

[a] No. of hydrogen bond donors.
[b] No. of hydrogen bond acceptors.
[c] All data from NIH PubChem except for ALogP (atom-based log of the partition coefficient), which were obtained from https://www.ebi.ac.uk/chembl/.

inhibitors fulfills all of the Ro5 criteria for oral bioavailability except for fedratinib, which has a molecular weight of 525 (Table 11).

5.2. The importance of lipophilicity and ligand efficiency

5.2.1. Lipophilic efficiency, LipE

Following the publication of Lipinski's Ro5 in 2001 [90], subsequent analyses of the physicochemical properties of orally effective agents have led to numerous extensions and refinements [91–98]. Lipophilic efficiency (LipE) is a feature that is used in drug discovery and development that combines drug affinity and lipophilic-driven binding as a method to characterize binding efficacy. The following formulas are used to compute lipophilic efficiency:

$$\text{LipE} = \text{pIC}_{50} - \text{ALogP};\ \text{LipE} = \text{p}K_\text{i} - \text{ALogP}$$

Similar to its usage to express the molar hydrogen ion concentration as pH, the mathematical operator p signifies the negative of the Log of the IC_{50} or K_i. Furthermore, ALogP is an atom-based computed Log of the partition coefficient; this value is the ratio of the drug content in the organic phase divided by its solubility in the aqueous phase of immiscible *n*-octanol/water.

The second term of the equation (– ALogP or minus ALogP) represents the lipophilicity of a ligand and the value is computed using an algorithm based upon the physicochemical properties of thousands of reference organic compounds. The greater the solubility of a drug in the organic phase of the two-phase *n*-octanol/water mixture, the greater is its lipophilicity, and the more it reduces the lipophilic efficiency value. Leeson and Springthorpe reported that ligand lipophilicity, as assessed by the – ALogP value, is one of the more important parameters that should be monitored during drug discovery and development [92]. Their use of – ALogP was based upon work performed before the application of the distribution coefficient (D) became more common. The distribution coefficient ($LogD_{7.4}$) represents the ratio of the content of the ionized and nonionized agent in the organic phase and the aqueous phase of immiscible *n*-octanol/phosphate buffer at pH 7.4. For practical purposes, either $LogD_{7.4}$ or ALogP can be used to compare a series of compounds during drug development. Hopkins et al. indicated that optimal values of lipophilic efficiency are greater than ~ 5; abrocitinib, baricitinib, ruxolitinib, and tofacitinib fall into this category (Table 12) [94]. These investigators also indicated that optimal values of LogP are less than ~ 3; abrocitinib, baricitinib, tofacitinib, and upadacitinib have this property. Note that a substance with a large negative (– ALogP) value decreases the lipophilic efficiency.

5.2.2. Ligand efficiency, LE

Ligand efficiency calculations are a procedure for comparing drug affinities based upon the average binding energy per atom. The ligand efficiency (LE) relates potency, or binding affinity, to the number of heavy (nonhydrogen) atoms of a compound. The following formula is used to calculate this value:

$$\text{LE} = \Delta G^{\circ\prime}/\text{N} = -\text{RT}\ \ln K_\text{eq}/\text{N} = -2{\cdot}303\text{RT}\ \text{Log}\ K_\text{eq}/\text{N}$$

$\Delta G^{\circ\prime}$ is the standard free energy change of a ligand binding to its target enzyme at neutral pH, R represents the universal gas constant, (1.98×10^{-3} kcal/degree-mol), T denotes the absolute temperature in degrees Kelvin, K_{eq} is the value of the equilibrium constant, and N is the number of nonhydrogen (heavy) atoms in the drug. Hopkins et al. suggested that values of ligand efficiency should be 0.3 kcal/mol or greater [91,94] and all of the FDA-approved JAK inhibitors except for pacritinib fulfill this criterion (Table 12). The IC_{50} or K_i values are proxies for the equilibrium constant. At a physiological temperature of 37 °C (310 K), this equation becomes $-(2.303 \times (1.98 \times 10^{-3}/\text{K}) \times 310\ \text{K}\ \text{Log}\ K_\text{eq})/\text{N}$ or $-1.41\ \text{Log}\ K_\text{eq}/\text{N}$. Other investigators use a temperature of 300 K and the multiplication factor is – 1.37 [64]. Ligand efficiency determinations are especially helpful in fragment-based drug discovery protocols and, like lipophilic efficiency, they help in the selection of congeners of lead compounds that may be useful for further development [95].

5.2.3. Additional chemical descriptors of orally effective drugs

To improve drug properties related to oral bioavailability, not unexpectedly, the Ro5 is associated with many corollaries. Veber et al. found, for example, that the polar surface area (PSA) and the number of rotatable bonds differentiates between orally active and inactive drugs for a large series of substances in rats [96]. They discovered that the number of rotatable bonds is generally 10 or less. This characteristic is believed to regulate passive membrane permeation and it reflects molecular flexibility (degrees of freedom). Moreover, the number of degrees of freedom correlates with the entropy change that accompanies drug binding. These authors found that orally effective medicinals have a polar surface area less than or equal to 140 $Å^2$. All of the FDA-approved JAK family inhibitors, except for fedratinib, have fewer than ten rotatable bonds and all of them have a polar surface area less than 140 $Å^2$ (Table 12). Moreover, Oprea found that the number of rings (both aromatic and nonaromatic) in most orally approved drugs is three or greater [97]. Except for abrocitinib and tofacitinib with two aromatic rings, the five other approved JAK-family blockers have three aromatic rings.

The molecular complexity of a medicinal agent is based upon its structural features, symmetry properties, and the elements it contains. The Bertz/Hendrickson/Ihlenfelt algorithm is used to calculate molecular complexity [99,100]. Complexity is related to the number and identity of the component atoms, the nature of the chemical bonds

Table 12
Properties of FDA-approved small molecule JAK-family kinase inhibitors.

Drug	Target, kinase family	K_i nM[a]	pK_i	ALogP[b]	LipE[c]	N[d]	LE[e]	Solubility, μg/ml[f]	Dosage, mg/day[g]	Log $D_{7.4}$[b]	nRb[h]	nAr[i]	Benzenes
Abrocitinib	JAK1	5.1	8.29	1.25	7.04	22	0.53	420	100	0.79	6	3	0
Baricitinib	JAK2/1	7	8.15	1.1	7.05	26	0.442	357	2	-0.19	5	3	0
Fedratinib	JAK2/3	6	8.22	4.82	3.40	37	0.313	9.49	400	3.23	11	3	2
Pacritinib	JAK2/TYK2	19	7.72	4.47	2.21	35	0.289	38.1	400 *	3.11	4	4	1
Ruxolitinib	JAK1/2	1.2	8.92	3.47	5.45	23	0.547	116	20 *	2.48	4	3	0
Tofacitinib	JAK1/2/3, TYK2	0.79	9.1	1.54	7.56	23	0.558	299	10 *	1.19	3	2	0
Upadacitinib	JAK1	43	7.37	2.91	4.46	27	0.385	70.7	15	0.85	3	3	0

[a] Representative values obtained from www.ebi.ac.μg/chembl/ and from klifs.net and they refer to the first target listed.
[b] Values for atom-based ALogP from https://www.ebi.ac.uk/chembl/
[c] $\text{LipE} = p\text{IC}_{50} - \text{ALogP}$
[d] N, Number of heavy atoms.
[e] $\text{LE} = -2.303\ \text{RT}\ \text{Log}_{10}\ K_i/\text{N}$ where N is the number of heavy (non-hydrogen) atoms in the drug.
[f] Values from https://go.drugbank.com/drugs/
[g] Dosage from FDA label; * , one-half of total daily dose taken twice per day.
[h] nRb, number of Rotatable bonds.
[i] nAr, number of Aromatic rings.

(single, double, triple, aromatic), and the bonding pattern. Molecular complexity values range from 0 for simple ions to several thousand for intricate natural products. Larger molecules usually have a higher molecular complexity value than smaller ones. The molecular complexity values for the medicinals in this article were acquired from PubChem (https://pubchem.ncbi.nlm.nih.gov/). Of the seven FDA-approved JAK-family antagonists, the values range from 453 for ruxolitinib to 787 for fedratinib (Table 12). These values fall within the range of the other FDA-approved protein kinase antagonists [101–104]. There are no optimal or recommended molecular complexity values for orally bioavailable medicinals; however, the value of this parameter may be helpful in determining the ease or difficulty in the synthesis of the drug, a significant consideration in the commercial production of pharmaceutical agents.

Ritchie and Macdonald examined the role of aromaticity as it relates to drug effectiveness [105]. Aromaticity refers to cyclically conjugated molecules such as pyrimidines with enhanced stability because of electron delocalization. These investigators considered bicyclic and tricyclic structures as containing two and three aromatic rings, respectively. The aromatic ring content includes structures with both carbon and heteroatom components. They found that increasing the number of carboaromatic rings has a detrimental effect on drug efficacy by inhibiting CYP450 (cytochrome p450), increasing binding to serum albumin, and decreasing aqueous solubility. The aromatic ring count of the seven approved JAK-family kinase inhibitors ranges from two to four. Fedratinib contains two benzene rings and pacritinib contains one. These values fall in the range of the other approved drugs [89].

Bayliss et al. evaluated the solubility, dosage, and lipophilicity for orally bioavailable drugs and drug candidates [106]. These authors suggested that drugs with an aqueous solubility of less than 100 μg/ml are associated with increased risk of failure during the drug development process. Three of the seven FDA-approved JAK family inhibitors have a solubility less than 100 μg/ml including fedratinib, pacritinib, and upadacitinib (Table 12). Their work indicated that dosages of 100 mg or less daily reduces the risk of toxicity. Of the seven approved JAK-family kinase inhibitors, only fedratinib and pacritinib – with daily doses of 400 mg – exceeds the 100 mg daily dosage cutoff value (Table 12).

6. Epilogue

Of all of the human protein kinases, only five contain both a pseudokinase and an active kinase: JAK1/2/3, TYK2, and EIF2AK4 (a serine/threonine protein kinase). The latter enzyme mediates the phosphorylation of eEF2 (eukaryotic protein synthesis elongation factor-2). RSK1/2/3/4, obscurin, and SPEG are protein-serine/threonine kinases that contain two active catalytic domains. The RSK (ribosomal protein 6 kinase) enzymes catalyze the phosphorylation of ribosomal proteins. Obscurin is the product of the *OBSCN* gene and consists of 7968 amino acid residues with a molecular mass of 868 kDa! This enzyme participates in myofibrillogenesis. SPEG is a striated muscle preferentially expressed gene that participates in muscle cell differentiation; it belongs to the myosin-light chain kinase family.

In 2022, the US FDA had approved 71 small molecule protein kinase inhibitors for the treatment of human diseases (supplementary material), nearly all of which are orally effective with the exception of temsirolimus (which is given intravenously) and netarsudil (which is given as an eye drop). Ruxolitinib is orally bioavailable, but it is also formulated as a cream for its topical application in the treatment of atopic dermatitis. Of the 71 approved small molecule protein kinase inhibitors, the majority (39) inhibit receptor protein-tyrosine kinases, 16 inhibit nonreceptor protein-tyrosine kinases, and 16 are directed at protein-serine/threonine protein kinases including the dual specificity protein kinases MEK1/2. Most of the approved drugs (62) are used in the treatment of patients with neoplasms. The FDA has also approved one protein kinase inhibitor (oclacitinib) for the treatment of canine dermatitis [48]. At least 18 of the approved drugs are multikinase inhibitors that block enzymes belonging to more than one family. This has advantages and disadvantages. It is possible that the therapeutic effectiveness of such drugs may be related to the inhibition of more than one enzyme. For example, sunitinib and cabozantinib have potent AXL off-target activity, which augments their clinical effectiveness [107]. Contrariwise, the blockade of nontarget enzymes may lead to various toxicities. Consequently, we have the rhetorical question of whether magic shotguns are to be favored over magic bullets [108].

A total of ten drugs is directed toward nonmalignancies; abrocitinib, ruxolitinib, and upadacitinib are used in the treatment of atopic dermatitis; baricitinib and tofacitinib are prescribed for the treatment of rheumatoid arthritis; upadacitinib is approved for the treatment of rheumatoid arthritis and psoriatic arthritis; fostamatinib is used for the treatment of chronic immune thrombocytopenia; nintedanib is prescribed for the treatment of idiopathic pulmonary fibrosis; sirolimus is used to prevent rejections following renal transplantation; belumosudil is prescribed for the treatment of graft vs. host disease; and netarsudil is used to treat glaucoma. Ruxolitinib is approved for the treatment of neoplastic (myelofibrosis and polycythemia) and nonneoplastic (atopic dermatitis) disorders.

Manning et al. reported that the human protein kinase super family consists of 518 members [4]. Because mutations and dysregulation of protein kinases play fundamental roles in the pathogenesis of many human diseases, this family of enzymes has become one of the most important drug targets over the past two decades [109,110]. Owing to the 244 disease loci and cancer amplicons that have been mapped in the human genome [4], it is likely that there will be a significant increase in the number of enzymes that will be studied for the treatment of many more illnesses. Possibilities include targeting JAK1 and JAK2 for the treatment of lupus erythematosus [111]; p38 MAP kinase for therapies directed toward asthma, atherosclerosis, Crohn disease, psoriasis, and rheumatoid arthritis [112]; Rho kinase for the treatment of hypertension, cerebral vasospasm, coronary vasospasm, myocardial infarction and heart failure [113]; glycogen synthase kinase-3β, Fyn, and DYRK1A for the treatment of Alzheimer disease [114]; protein kinase R-like endoplasmic reticulum kinase (PERK) for therapies directed toward Alzheimer disease, Parkinson disease, Huntington disease, and amyotrophic lateral sclerosis [115]; protein kinase Cα for colon, skin, endometrial, breast, and lung cancers [116]; and Pkn3 as a therapy for osteoporosis [117]. In the early days of protein kinase research, the prevailing notion was that these enzymes played an important role in hormone action; we now see that protein kinases have a much wider field of action [10].

Conflict of interest

The author is unaware of any affiliations, memberships, or financial holdings that might be perceived as affecting the objectivity of this review.

Data Availability

All data are taken from the literature.

Acknowledgment

I thank Dr. Albert J. Kooistra for providing the data in Tables 6 and 7 and the template depicted in Fig. 5. I acknowledge the editorial and bibliographic assistance provided by Laura M. Roskoski. I also thank Jasper Martinsek and Josie Rudnicki for their role in preparing the figures and W.S. Sheppard and Pasha Brezina for their help in structural analyses. The colored figures in this paper were evaluated to ensure that their perception was accurately conveyed to colorblind readers [118].

Appendix A. Supporting information

Supplementary data associated with this article can be found in the online version at doi:10.1016/j.phrs.2022.106362.

References

[1] N.K. Williams, R.S. Bamert, O. Patel, C. Wang, P.M. Walden, A.F. Wilks, E. Fantino, J. Rossjohn, I.S. Lucet, Dissecting specificity in the Janus kinases: the structures of JAK-specific inhibitors complexed to the JAK1 and JAK2 protein tyrosine kinase domains, J. Mol. Biol. 387 (2009) 219–232.

[2] A.F. Wilks, The JAK kinases: not just another kinase drug discovery target, Semin Cell Dev. Biol. 19 (2008) 319–328.

[3] M. Kawamura, D.W. McVicar, J.A. Johnston, T.B. Blake, Y.Q. Chen, B.K. Lal, A. R. Lloyd, D.J. Kelvin, J.E. Staples, J.R. Ortaldo, J.J. O'Shea, Molecular cloning of L-JAK, a Janus family protein-tyrosine kinase expressed in natural killer cells and activated leukocytes, Proc. Natl. Acad. Sci. USA 91 (1994) 6374–6378.

[4] G. Manning, D.B. Whyte, R. Martinez, T. Hunter, S. Sudarsanam, The protein kinase complement of the human genome, Science 298 (2002) 1912–1934.

[5] X. Hu, J. Li, M. Fu, X. Zhao, W. Wang, The JAK/STAT signaling pathway: from bench to clinic, Signal Transduct. Target Ther. 6 (2021) 402, https://doi.org/10.1038/s41392-021-00791-1.

[6] B.F. Haynes, K.A. Soderberg, A.S. Fauci, Introduction to the immune system, in: J. Loscalzo, A.S. Fauci, D.L. Kasper, S.L. Hauser, D.L. Longo, J.L. Jameson (Eds.), Harrison's Principles of Internal Medicine, 21st edition.,, McGraw Hill Medical, New York, 2022, pp. 2671–2701.

[7] J.J. Babon, I.S. Lucet, J.M. Murphy, N.A. Nicola, L.N. Varghese, The molecular regulation of Janus kinase (JAK) activation, Biochem J. 462 (2014) 1–13.

[8] S. Abroun, N. Saki, M. Ahmadvand, F. Asghari, F. Salari, F. Rahim, STATs: An old story, yet mesmerizing, Cell J. l (17) (2015) 395–411.

[9] X. Chen, U. Vinkemeier, Y. Zhao, D. Jeruzalmi, J.E. Darnell Jr, J. Kuriyan, Crystal structure of a tyrosine phosphorylated STAT-1 dimer bound to DNA, Cell 93 (1998) 827–839.

[10] R. Roskoski Jr., A historical overview of protein kinases and their targeted small molecule inhibitors, Pharm. Res 100 (2015) 1–23.

[11] J. Irie-Sasaki, T. Sasaki, W. Matsumoto, A. Opavsky, M. Cheng, G. Welstead, E. Griffiths, C. Krawczyk, C.D. Richardson, K. Aitken, N. Iscove, G. Koretzky, P. Johnson, P. Liu, D.M. Rothstein, J.M. Penninger, CD45 is a JAK phosphatase and negatively regulates cytokine receptor signalling, Nature 18 (409) (2001) 349–354.

[12] K. Yamaoka, P. Saharinen, M. Pesu, V.E. Holt 3rd, O. Silvennoinen, J.J. O'Shea, The Janus kinases (Jaks), Genome Biol. 5 (2004) 253.

[13] D.R. Knighton, J.H. Zheng, L.F. Ten Eyck, V.A. Ashford, N.H. Xuong, S.S. Taylor, J.M. Sowadski, Crystal structure of the catalytic subunit of cyclic adenosine monophosphate-dependent protein kinase, Science 253 (1991) 407–414.

[14] D.R. Knighton, J.H. Zheng, L.F. Ten Eyck, N.H. Xuong, S.S. Taylor, J.M. Sowadski, Structure of a peptide inhibitor bound to the catalytic subunit of cyclic adenosine monophosphate-dependent protein kinase, Science 253 (1991) 414–420.

[15] S.S. Taylor, M.M. Keshwani, J.M. Steichen, A.P. Kornev, Evolution of the eukaryotic protein kinases as dynamic molecular switches, Philos. Trans. R. Soc. Lond. B Biol. Sci. 367 (2012) 2517–2528.

[16] S.K. Hanks, T. Hunter, Protein kinases 6. The eukaryotic protein kinase superfamily: kinase (catalytic) domain structure and classification, FASEB J. 9 (1995) 576–596.

[17] H.S. Meharena, P. Chang, M.M. Keshwani, K. Oruganty, A.K. Nene, N. Kannan, S. S. Taylor, A.P. Kornev, Deciphering the structural basis of eukaryotic protein kinase regulation, PLoS Biol. 11 (2013), e1001680.

[18] S.R. Hubbard, J.H. Till, Protein tyrosine kinase structure and function, Annu Rev. Biochem 69 (2000) 373–398, https://doi.org/10.1146/annurev.biochem.69.1.373.

[19] K. Chatti, W.L. Farrar, R.J. Duhé, Tyrosine phosphorylation of the Janus kinase 2 activation loop is essential for a high-activity catalytic state but dispensable for a basal catalytic state, Biochemistry 43 (2004) 4272–4283.

[20] A.P. Kornev, N.M. Haste, S.S. Taylor, L.F. Ten Eyck, Surface comparison of active and inactive protein kinases identifies a conserved activation mechanism, Proc. Natl. Acad. Sci. USA 103 (2006) 17783–17788.

[21] A.P. Kornev, S.S. Taylor, L.F. Ten Eyck, A helix scaffold for the assembly of active protein kinases, Proc. Natl. Acad. Sci. USA 105 (2008) 14377–14382.

[22] R. Roskoski Jr., Classification of small molecule protein kinase inhibitors based upon the structures of their drug-enzyme complexes, Pharm. Res 103 (2016) 26–48.

[23] R. Roskoski Jr., Anaplastic lymphoma kinase (ALK): structure, oncogenic activation, and pharmacological inhibition, Pharm. Res 68 (2013) 68–94 (doi:).

[24] R. Roskoski Jr., Anaplastic lymphoma kinase (ALK) inhibitors in the treatment of ALK-driven lung cancers, Pharm. Res 117 (2017) 343–356, https://doi.org/10.1016/j.phrs.2017.01.007.

[25] R. Roskoski Jr., The preclinical profile of crizotinib in the treatment of non-small cell lung cancer and other neoplastic disorders, Expert Opin. Drug Dis. 8 (2013) 1165–1179, https://doi.org/10.1517/17460441.2013.813015.

[26] R. Roskoski Jr., The ErbB/HER family of protein-tyrosine kinases and cancer, Pharm. Res 79 (2014) 34–74, https://doi.org/10.1016/j.phrs.2013.11.002, 10.1016/j.phrs.2012.11.007.

[27] R. Roskoski Jr., ErbB/HER protein-tyrosine kinases: structure and small molecule inhibitors, Pharm. Res 87 (2014) 42–59, https://doi.org/10.1016/j.phrs.2014.06.001.

[28] R. Roskoski Jr., Small molecule inhibitors targeting the EGFR/ErbB family of protein-tyrosine kinases in human cancers, Pharm. Res 139 (2019) 395–411, https://doi.org/10.1016/j.phrs.2018.11.014.

[29] R. Roskoski Jr., The role of small molecule platelet-derived growth factor receptor (PDGFR) inhibitors in the treatment of neoplastic disorders, Pharm. Res 129 (2018) 65–83, https://doi.org/10.1016/j.phrs.2018.01.021.

[30] R. Roskoski Jr., The role of small molecule Kit protein-tyrosine kinase inhibitors in the treatment of neoplastic disorders, Pharm. Res 133 (2018) 35–52, https://doi.org/10.1016/j.phrs.2018.04.020.

[31] R. Roskoski Jr., Vascular endothelial growth factor (VEGF) and VEGF receptor inhibitors in the treatment of renal cell carcinomas, Pharm. Res 120 (2017) 116–132, https://doi.org/10.1016/j.phrs.2017.03.010.

[32] R. Roskoski Jr., The role of fibroblast growth factor receptor (FGFR) protein-tyrosine kinase inhibitors in the treatment of cancers including those of the urinary bladder, Pharm. Res 151 (2020), 104567, https://doi.org/10.1016/j.phrs.2019.104567.

[33] R. Roskoski Jr., The role of small molecule Flt3 receptor protein-tyrosine kinase inhibitors in the treatment of Flt3-positive acute myelogenous leukemias, Pharm. Res 155 (2020), 104725, https://doi.org/10.1016/j.phrs.2020.104725.

[34] R. Roskoski Jr., A. Sadeghi-Nejad, Role of RET protein-tyrosine kinase inhibitors in the treatment RET-driven thyroid and lung cancers, Pharm. Res 128 (2018) 1–17, https://doi.org/10.1016/j.phrs.2017.12.021.

[35] R. Roskoski Jr., ROS1 protein-tyrosine kinase inhibitors in the treatment of ROS1 fusion protein-driven non-small cell lung cancers, Pharm. Res 121 (2017) 202–212, https://doi.org/10.1016/j.phrs.2017.04.022.

[36] R. Roskoski Jr., Ibrutinib inhibition of Bruton protein-tyrosine kinase (BTK) in the treatment of B cell neoplasms, Pharm. Res 113 (2016) 395–408, https://doi.org/10.1016/j.phrs.2016.09.011.

[37] R. Roskoski Jr., Src protein-tyrosine kinase structure, mechanism, and small molecule inhibitors, Pharm. Res 94 (2015) 9–25, https://doi.org/10.1016/j.phrs.2015.01.003.

[38] M.C. Frame, R. Roskoski Jr., Src Family Tyrosine Kinases. Reference module in life sciences, Elsevier, Amsterdam, 2017, pp. 1–11, https://doi.org/10.1016/B978-0-12-809633-8.07199-5.

[39] R. Roskoski Jr., MEK1/2 dual-specificity protein kinases: structure and regulation, Biochem Biophys. Res Commun. 417 (2012) 5–10, https://doi.org/10.1016/j.bbrc.2011.11.145.

[40] R. Roskoski Jr., Allosteric MEK1/2 inhibitors including cobimetanib and trametinib in the treatment of cutaneous melanomas, Pharm. Res 117 (2017) 20–31, https://doi.org/10.1016/j.phrs.2016.12.009.

[41] R. Roskoski Jr., Cyclin-dependent protein kinase inhibitors including palbociclib as anticancer drugs, Pharm. Res 107 (2016) 249–275, https://doi.org/10.1016/j.phrs.2016.03.012.

[42] R. Roskoski Jr., Cyclin-dependent protein serine/threonine kinase inhibitors as anticancer drugs, Pharm. Res 139 (2019) 471–488.

[43] R. Roskoski Jr., RAF protein-serine/threonine kinases: structure and regulation, Biochem Biophys. Res Commun. 399 (2010) 313–317, https://doi.org/10.1016/j.bbrc.2010.07.092.

[44] R. Roskoski Jr., Targeting oncogenic Raf protein-serine/threonine kinases in human cancers, Pharm. Res 135 (2018) 239–258, https://doi.org/10.1016/j.phrs.2018.08.013.

[45] R. Roskoski Jr., ERK1/2 MAP kinases: structure, function, and regulation, Pharm. Res 66 (2012) 105–143, https://doi.org/10.1016/j.phrs.2012.04.005.

[46] R. Roskoski Jr., Targeting ERK1/2 protein-serine/threonine kinases in human cancers, Pharm. Res 142 (2019) 151–168, https://doi.org/10.1016/j.phrs.2019.01.039.

[47] R. Roskoski Jr., Properties of FDA-approved small molecule phosphatidylinositol 3-kinase inhibitors prescribed for the treatment of malignancies, Pharm. Res 168 (2021), 105579, https://doi.org/10.1016/j.phrs.2021.105579.

[48] R. Roskoski Jr., Janus kinase (JAK) inhibitors in the treatment of inflammatory and neoplastic diseases, Pharm. Res 111 (2016) 784–803, https://doi.org/10.1016/j.phrs.2016.07.038.

[49] C.R. Glassman, N. Tsutsumi, R.A. Saxton, P.J. Lupardus, K.M. Jude, K.C. Garcia, Structure of a Janus kinase cytokine receptor complex reveals the basis for dimeric activation, Science 376 (2022) 163–169, https://doi.org/10.1126/science.abn8933.

[50] H.M. Hammarén, A.T. Virtanen, J. Raivola, O. Silvennoinen, The regulation of JAKs in cytokine signaling and its breakdown in disease, Cytokine 118 (2019) 48–63, https://doi.org/10.1016/j.cyto.2018.03.041.].

[51] C. Recio, H. Aranda-Tavío, M. Guerra-Rodríguez, M. de Mirecki-Garrido, P. Martín-Rodríguez, B. Guerra, L. Fernández-Pérez, JAK, oncokinase Hematol. Cancer (2019), https://doi.org/10.5772/intechopen.79884.

[52] P.J. Lupardus, M. Ultsch, H. Wallweber, P. Bir Kohli, A.R. Johnson, C. Eigenbrot, Structure of the pseudokinase-kinase domains from protein kinase TYK2 reveals a mechanism for Janus kinase (JAK) autoinhibition, Proc. Natl. Acad. Sci. USA 111 (2014) 8025–8030.

[53] L. Springuel, J.C. Renauld, L. Knoops, JAK kinase targeting in hematologic malignancies: a sinuous pathway from identification of genetic alterations towards clinical indications, Haematologica 100 (2015) 1240–1253.

[54] B. Rah, R.A. Rather, G.R. Bhat, A.B. Baba, I. Mushtaq, M. Farooq, T. Yousuf, S. B. Dar, S. Parveen, R. Hassan, F. Mohammad, I. Qassim, A. Bhat, S. Ali, M. H. Zargar, D. Afroze, JAK/STAT signaling: molecular targets, therapeutic

opportunities, and limitations of targeted inhibitions in solid malignancies, Front Pharm. 13 (2022), 821344, https://doi.org/10.3389/fphar.2022.821344.
[55] A.C. Dar, K.M. Shokat, The evolution of protein kinase inhibitors from antagonists to agonists of cellular signaling, Annu Rev. Biochem 80 (2011) 769–795.
[56] F. Zuccotto, E. Ardini, E. Casale, M. Angiolini, Through the "gatekeeper door": exploiting the active kinase conformation, J. Med Chem. 53 (2010) 2691–2694.
[57] L.K. Gavrin, E. Saiah, Approaches to discover non-ATP site inhibitors, Med Chem. Commun. 4 (2013) 41.
[58] V. Lamba, I. Ghosh, New directions in targeting protein kinases: focusing upon true allosteric and bivalent inhibitors, Curr. Pharm. Des. 18 (2012) 2936–2945.
[59] R. Roskoski Jr., Orally effective FDA-approved protein kinase targeted covalent inhibitors (TCIs), Pharm. Res 165 (2021), 105422, https://doi.org/10.1016/j.phrs.2021.105422.
[60] V. Modi, R.L. Dunbrack, Kincore: a web resource for structural classification of protein kinases and their inhibitors, Nucleic Acids Res 50 (D1) (2022) D654–D664, https://doi.org/10.1093/nar/gkab920.
[61] J.J. Liao, Molecular recognition of protein kinase binding pockets for design of potent and selective kinase inhibitors, J. Med Chem. 50 (2007) 409–424.
[62] O.P. van Linden, A.J. Kooistra, R. Leurs, I.J. de Esch, C. de Graaf, KLIFS: a knowledge-based structural database to navigate kinase-ligand interaction space, J. Med Chem. 57 (2014) 249–277.
[63] G.K. Kanev, C. de Graaf, B.A. Westerman, I.J.P. de Esch, A.J. Kooistra, KLIFS: an overhaul after the first 5 years of supporting kinase research, Nucleic Acids Res (2020) gkaa895, https://doi.org/10.1093/nar/gkaa895.
[64] F. Carles, S. Bourg, C. Meyer, P. Bonnet, PKIDB: a curated, annotated and updated database of protein kinase inhibitors in clinical trials, Molecules 23 (4) (2018) pii: E908, https://doi.org/10.3390/molecules23040908.
[65] E.D. Deeks, S. Duggan, Abrocitinib: first approval, Drugs 81 (2021) 2149–2157, https://doi.org/10.1007/s40265-021-01638-3. Corrigendum: Drugs. 2022;82: 609. doi: 10.1007/s40265-022-01694-3.
[66] A. Coricello, F. Mesiti, A. Lupia, A. Maruca, S. Alcaro, Inside perspective of the synthetic and computational toolbox of JAK Inhibitors: recent updates, Molecules 25 (2020) 3321, https://doi.org/10.3390/molecules25153321.
[67] A. Markham, Baricitinib: first global approval, Drugs 77 (2017) 697–704, https://doi.org/10.1007/s40265-017-0723-3.
[68] R. Rubin, Baricitinib is first approved covid-19 immunomodulatory treatment, JAMA 327 (2022) 2281, https://doi.org/10.1001/jama.2022.9846.
[69] H.A. Blair, Fedratinib: first approval, Drugs 79 (2019) 1719–1725.
[70] K. Pettit, A. Rezazadeh, E.L. Atallah, J. Radich, Management of myeloproliferative neoplasms in the molecular era: from research to practice, Am. Soc. Clin. Oncol. Educ. Book 42 (2022) 1–19, https://doi.org/10.1200/EDBK_349615.
[71] J. Mascarenhas, R. Hoffman, Ruxolitinib: the first FDA approved therapy for the treatment of myelofibrosis, Clin. Cancer Res 18 (2012) 3008–3014, https://doi.org/10.1158/1078-0432.CCR-11-3145.
[72] L.A. Raedler, Jakafi (Ruxolitinib): first FDA-approved medication for the treatment of patients with polycythemia vera, Am. Health Drug Benefits 8 (2015) 75–79.
[73] W. Yang, G. Zhu, M. Qin, Z. Li, B. Wang, J. Yang, T. Wang, The effectiveness of ruxolitinib for acute/chronic graft-versus-host disease in children: a retrospective study, Drug Des. Devel Ther. 15 (2021) 743–752, https://doi.org/10.2147/DDDT.S287218.
[74] C.C. Ayala-Aguilera, T. Valero, Á. Lorente-Macías, D.J. Baillache, S. Croke, A. Unciti-Broceta, small molecule kinase inhibitor drugs (1995-2021): medical indication, pharmacology, and synthesis, J. Med Chem. 65 (2022) 1047–1131, https://doi.org/10.1021/acs.jmedchem.1c00963.
[75] M.M. Kostik, R.K. Raupov, E.N. Suspitsin, E.A. Isupova, E.V. Gaidar, T. V. Gabrusskaya, M.A. Kaneva, L.S. Snegireva, T.S. Likhacheva, R.S. Miulkidzhan, A.V. Kosmin, A.V. Tumakova, V.V. Masalova, M.F. Dubko, O.V. Kalashnikova, I. Aksentijevich, V.G. Chasnyk, the safety and efficacy of tofacitinib in 24 cases of pediatric rheumatic diseases: single centre experience, Front Pediatr 10 (2022), 820586, https://doi.org/10.3389/fped.2022.820586.
[76] R. Mohanakrishnan, S. Beier, A. Deodhar, Tofacitinib for the treatment of active ankylosing spondylitis in adults, Expert Rev. Clin. Immunol. 18 (2022) 273–280, https://doi.org/10.1080/1744666X.2022.2038134.
[77] S. Duggan, S.J. Keam, Upadacitinib: first approval, Drugs 79 (2019) 1819–1828, https://doi.org/10.1007/s40265-019-01211-z.
[78] E. Muensterman, B. Engelhardt, S. Gopalakrishnan, J.K. Anderson, M. F. Mohamed, Upadacitinib pharmacokinetics and exposure-response analyses of efficacy and safety in psoriatic arthritis patients - Analyses of phase III clinical trials, Clin. Transl. Sci. 15 (2022) 267–278, https://doi.org/10.1111/cts.13146.
[79] S. Narla, J.I. Silverberg, The suitability of treating atopic dermatitis with Janus kinase inhibitors, Expert Rev. Clin. Immunol. 18 (2022) 439–459, https://doi.org/10.1080/1744666X.2022.2060822.
[80] M. Napolitano, F. D'Amico, E. Ragaini, L. Peyrin-Biroulet, S. Danese, Evaluating upadacitinib in the treatment of moderate-to-severe active ulcerative colitis: design, development, and potential position in therapy, Drug Des. Devel Ther. 16 (2022) 1897–1913, https://doi.org/10.2147/DDDT.S340459.
[81] A.M. Shawky, F.A. Almalki, A.N. Abdalla, A.H. Abdelazeem, A.M. Gouda, A comprehensive overview of globally approved JAK inhibitors, Pharmaceutics 14 (2022) 1001, https://doi.org/10.3390/pharmaceutics14051001.
[82] M.L. Vazquez, N. Kaila, J.W. Strohbach, J.D. Trzupek, M.F. Brown, M. E. Flanagan, M.J. Mitton-Fry, T.A. Johnson, R.E. TenBrink, E.P. Arnold, A. Basak, S.E. Heasley, S. Kwon, J. Langille, M.D. Parikh, S.H. Griffin, J.M. Casavant, B. A. Duclos, A.E. Fenwick, T.M. Harris, S. Han, N. Caspers, M.E. Dowty, X. Yang, M. E. Banker, M. Hegen, P.T. Symanowicz, L. Li, L. Wang, T.H. Lin, J. Jussif, J. D. Clark, J.B. Telliez, R.P. Robinson, R. Unwalla, Identification of N-{cis-3-[Methyl(7H-pyrrolo[2,3-*d*]pyrimidin-4-yl)amino]cyclobutyl}propane-1-sulfonamide (PF-04965842): a selective JAK1 clinical candidate for the treatment of autoimmune diseases, J. Med Chem. 61 (2018) 1130–1152, https://doi.org/10.1021/acs.jmedchem.7b01598.
[83] M. Nogueira, T. Torres, Janus Kinase inhibitors for the treatment of atopic dermatitis: focus on abrocitinib, baricitinib, and upadacitinib, Dermatol. Pr. Concept 11 (2021), e2021145, https://doi.org/10.5826/dpc.1104a145.
[84] Y. Chang, J. Min, J.A. Jarusiewicz, M. Actis, S. Yu-Chen Bradford, A. Mayasundari, L. Yang, D. Chepyala, L.J. Alcock, K.G. Roberts, S. Nithianantham, D. Maxwell, L. Rowland, R. Larsen, A. Seth, H. Goto, T. Imamura, K. Akahane, B.S. Hansen, S.M. Pruett-Miller, E.M. Paietta, M. R. Litzow, C. Qu, J.J. Yang, M. Fischer, Z. Rankovic, C.G. Mullighan, Degradation of Janus kinases in CRLF2-rearranged acute lymphoblastic leukemia, Blood 138 (2021) 2313–2326, https://doi.org/10.1182/blood.2020006846.
[85] P.J. Richardson, B.W.S. Robinson, D.P. Smith, J. Stebbing, The AI-assisted identification and clinical efficacy of baricitinib in the treatment of COVID-19, Vaccin. (Basel) 10 (2022) 951, https://doi.org/10.3390/vaccines10060951.
[86] R.R. Davis, B. Li, S.Y. Yun, A. Chan, P. Nareddy, S. Gunawan, M. Ayaz, H. R. Lawrence, G.W. Reuther, N.J. Lawrence, E. Schönbrunn, Structural insights into JAK2 inhibition by ruxolitinib, fedratinib, and derivatives thereof, J. Med Chem. 64 (2021) 2228–2241, https://doi.org/10.1021/acs.jmedchem.0c01952.
[87] N.K. Williams, R.S. Bamert, O. Patel, C. Wang, P.M. Walden, A.F. Wilks, E. Fantino, J. Rossjohn, I.S. Lucet, Dissecting specificity in the Janus kinases: the structures of JAK-specific inhibitors complexed to the JAK1 and JAK2 protein tyrosine kinase domains, J. Mol. Biol. 387 (2009) 219–232, https://doi.org/10.1016/j.jmb.2009.01.041.
[88] J.E. Chrencik, A. Patny, I.K. Leung, B. Korniski, T.L. Emmons, T. Hall, R. A. Weinberg, J.A. Gormley, J.M. Williams, J.E. Day, J.L. Hirsch, J.R. Kiefer, J. W. Leone, H.D. Fischer, C.D. Sommers, H.C. Huang, E.J. Jacobsen, R.E. Tenbrink, A.G. Tomasselli, T.E. Benson, Structural and thermodynamic characterization of the TYK2 and JAK3 kinase domains in complex with CP-690550 and CMP-6, J. Mol. Biol. 400 (2010) 413–433, https://doi.org/10.1016/j.jmb.2010.05.020.
[89] R. Roskoski Jr., Hydrophobic and polar interactions of FDA-approved small molecule protein kinase inhibitors with their target enzymes, Pharm. Res 169 (2021), 105660, https://doi.org/10.1016/j.phrs.2021.105660.
[90] C.A. Lipinski, F. Lombardo, B.W. Dominy, P.J. Feeney, Experimental and computational approaches to estimate solubility and permeability in drug discovery and development settings, Adv. Drug Deliv. Rev. 46 (2001) 3–26, https://doi.org/10.1016/s0169-409x(00)00129-0.
[91] A.L. Hopkins, C.R. Groom, A. Alex, Ligand efficiency: a useful metric for lead selection, Drug Disco Today 9 (2004) 430–431, https://doi.org/10.1016/S1359-6446(04)03069-7.
[92] P.D. Leeson, B. Springthorpe, The influence of drug-like concepts on decision-making in medicinal chemistry, Nat. Rev. Drug Disco 6 (2007) 881–890, https://doi.org/10.1038/nrd2445.
[93] S. Ekins, N.K. Litterman, C.A. Lipinski, B.A. Bunin, Thermodynamic proxies to compensate for biases in drug discovery methods, Pharm. Res 33 (2016) 194–205, https://doi.org/10.1007/s11095-015-1779-y.
[94] A.L. Hopkins, G.M. Keserü, P.D. Leeson, D.C. Rees, C.H. Reynolds, The role of ligand efficiency metrics in drug discovery, Nat. Rev. Drug Disco 13 (2014) 105–121, https://doi.org/10.1038/nrd4163.
[95] P.D. Leeson, Molecular inflation, attrition, and the rule of five, Adv. Drug Deliv. Rev. 101 (2016) 22–33, https://doi.org/10.1016/j.addr.2016.01.018.
[96] D.F. Veber, S.R. Johnson, H.Y. Cheng, B.R. Smith, K.W. Ward, K.D. Kopple, Molecular properties that influence the oral bioavailability of drug candidates, J. Med Chem. 45 (2002) 2615–2623, https://doi.org/10.1021/jm020017n.
[97] T.I. Oprea, Property distribution of drug-related chemical databases, J. Comput. Aided Mol. Des. 14 (2000) 251–264, https://doi.org/10.1023/a:1008130001697.
[98] P.D. Leeson, A.P. Bento, A. Gaulton, A. Hersey, E.J. Manners, C.J. Radoux, A. R. Leach, Target-based evaluation of "drug-like" properties and ligand efficiencies, J. Med Chem. 64 (2021) 7210–7230, https://doi.org/10.1021/acs.jmedchem.1c00416.
[99] S.H. Bertz, The first general index of molecular complexity, J. Am. Chem. Soc. 1103 (1981) 3559–3601.
[100] J.B. Hendrickson, P. Huang, A.G. Toczko, Molecular complexity: a simplified formula adapted to individual atoms, J. Chem. Inf. Compout Sci. 27 (1987) 63–67.
[101] R. Roskoski Jr., Properties of FDA-approved small molecule protein kinase inhibitors: a 2020 update, Pharm. Res 152 (2020), 104609, https://doi.org/10.1016/j.phrs.2019.104609.
[102] R. Roskoski Jr., Properties of FDA-approved small molecule protein kinase inhibitors: a 2021 update, Pharm. Res 165 (2021), 105463, https://doi.org/10.1016/j.phrs.2021.105463.
[103] R. Roskoski Jr., Properties of FDA-approved small molecule protein kinase inhibitors: a 2022 update, Pharm. Res 175 (2022), 106037, https://doi.org/10.1016/j.phrs.2021.106037.
[104] R. Roskoski Jr., Targeting BCR-Abl in the treatment of Philadelphia-chromosome positive chronic myelogenous leukemia, Pharm. Res 178 (2022), 106156, https://doi.org/10.1016/j.phrs.2022.106156.
[105] T.J. Ritchie, S.J. Macdonald, Physicochemical descriptors of aromatic character and their use in drug discovery, J. Med Chem. 57 (2014) 7206–7215, https://doi.org/10.1021/jm500515d.
[106] M.K. Bayliss, J. Butler, P.L. Feldman, D.V. Green, P.D. Leeson, M.R. Palovich, A. J. Taylor, Quality guidelines for oral drug candidates: dose, solubility and

lipophilicity, Drug Disco Today 21 (2016) 1719–1727, https://doi.org/10.1016/j.drudis.2016.07.007.
[107] S.H. Myers, V.G. Brunton, A. Unciti-Broceta, AXL inhibitors in cancer: a medicinal chemistry perspective, J. Med Chem. 59 (2016) 3593–3608.
[108] B.L. Roth, D.J. Sheffler, W.K. Kroeze, Magic shotguns versus magic bullets: selectively non-selective drugs for mood disorders and schizophrenia, Nat. Rev. Drug Disco 3 (2004) 353–359.
[109] P. Cohen, D. Cross, P.A. Jänne, Kinase drug discovery 20 years after imatinib: progress and future directions, Nat. Rev. Drug Disco 20 (2021) 551–569, https://doi.org/10.1038/s41573-021-00195-4.
[110] M.M. Attwood, D. Fabbro, A.V. Sokolov, S. Knapp, H.B. Schiöth, Trends in kinase drug discovery: targets, indications and inhibitor design, Nat. Rev. Drug Disco 20 (2021) 839–861, https://doi.org/10.1038/s41573-021-00252-y. Author correction. Nat Rev Drug Discov 2021;20:798. doi: 10.1038/s41573-021-00303-4.
[111] C.C. Mok, The jakinibs in systemic lupus erythematosus: progress and prospects, Expert Opin. Invest. Drugs 28 (2019) 85–92.
[112] D.M. Goldstein, A. Kuglstatter, Y. Lou, M.J. Soth, Selective p38α inhibitors clinically evaluated for the treatment of chronic inflammatory disorders, J. Med Chem. 53 (2010) 2345–2353.
[113] K. Budzyn, P.D. Marley, C.G. Sobey, Targeting Rho and Rho-kinase in the treatment of cardiovascular disease, Trends Pharm. Sci. 27 (2006) 97–104.
[114] S. Demuro, R.M.C. Di Martino, J.A. Ortega, A. Cavalli, GSK-3β, FYN, and DYRK1A: master regulators in neurodegenerative pathways, Int J. Mol. Sci. 22 (2021) 9098, https://doi.org/10.3390/ijms22169098.
[115] T. Shacham, C. Patel, G.Z. Lederkremer, PERK pathway and neurodegenerative disease: to inhibit or to activate? Biomolecules 11 (2021) 354, https://doi.org/10.3390/biom11030354.
[116] A.R. Black, J.D. Black, The complexities of PKCα signaling in cancer, Adv. Biol. Regul. 80 (2021), 100769, https://doi.org/10.1016/j.jbior.2020.100769.
[117] S. Uehara, N. Udagawa, Y. Kobayashi, Regulation of osteoclast function via Rho-Pkn3-c-Src pathways, J. Oral. Biosci. 61 (2019) 135–140, https://doi.org/10.1016/j.job.2019.07.002.
[118] R. Roskoski Jr., Guidelines for preparing color figures for everyone including the colorblind, Erratum in: Pharmacol Res. 2018. pii: S1043-6618(18)31424-5, Pharm. Res 119 (2017) 240–241, https://doi.org/10.1016/j.phrs.2018.09.019.